EUROPEAN ORGANIZATION FOR NUCLEAR RESEARCH

CERN–EP/2000-111
27 July 2000

MEASUREMENT OF THE Λ POLARIZATION IN ν_μ CHARGED CURRENT INTERACTIONS IN THE NOMAD EXPERIMENT

NOMAD Collaboration

P. Astier[1)], D. Autiero[2)], A. Baldisseri[3)], M. Baldo-Ceolin[4)], M. Banner[1)], G. Bassompierre[5)], K. Benslama[6)], N. Besson[3)], I. Bird[2,6)], B. Blumenfeld[7)], F. Bobisut[4)], J. Bouchez[3)], S. Boyd[8)], A. Bueno[9,10)], S. Bunyatov[11)], L. Camilleri[2)], A. Cardini[12)], P.W. Cattaneo[13)], V. Cavasinni[14)], A. Cervera-Villanueva[2,15)], A. Chukanov[11)], G.M. Collazuol[4)], G. Conforto[2,16)], C. Conta[13)], M. Contalbrigo[4)], R. Cousins[12)], D. Daniels[9)], H. Degaudenzi[6)], T. Del Prete[14)], A. De Santo[2)], T. Dignan[9)], L. Di Lella[2)], E. do Couto e Silva[2)], J. Dumarchez[1)], M. Ellis[8)], T. Fazio[5)], G.J. Feldman[9)], R. Ferrari[13)], D. Ferrère[2)], V. Flaminio[14)], M. Fraternali[13)], J-M. Gaillard[5)], E. Gangler[1,2)], A. Geiser[2,17)], D. Geppert[17)], D. Gibin[4)], S. Gninenko[2,18)], A. Godley[8)], J-J. Gomez-Cadenas[2,15)], J. Gosset[3)], C. Gößling[17)], M. Gouanère[5)], A. Grant[2)], G. Graziani[19)], A. Guglielmi[4)], C. Hagner[3)], J. Hernando[15)], D. Hubbard[9)], P. Hurst[9)], N. Hyett[20)], E. Iacopini[19)], C. Joseph[6)], F. Juget[6)], M. Kirsanov[18)], O. Klimov[11)], J. Kokkonen[2)], A. Kovzelev[13,18)], A. Krasnoperov[5,11)], D. Kustov[11)], V. Kuznetsov[2,11)], S. Lacaprara[4)], C. Lachaud[1)], B. Lakić[21)], A. Lanza[13)], L. La Rotonda[22)], M. Laveder[4)], A. Letessier-Selvon[1)], J-M. Levy[1)], L. Linssen[2)], A. Ljubičić[21)], J. Long[7)], A. Lupi[19)], A. Marchionni[19)], F. Martelli[16)], X. Méchain[3)], J-P. Mendiburu[5)], J-P. Meyer[3)], M. Mezzetto[4)], S.R. Mishra[9,23)], G.F. Moorhead[20)], D. Naumov[11)], P. Nédélec[5)], Yu. Nefedov[11)], C. Nguyen-Mau[6)], D. Orestano[24)], F. Pastore[24)], L.S. Peak[8)], E. Pennacchio[16)], H. Pessard[5)], R. Petti[2,13)], A. Placci[2)], G. Polesello[13)], D. Pollmann[17)], A. Polyarush[18)], B. Popov[1,11)], C. Poulsen[20)], P. Rathouit[3)], J. Rico[10)], P. Riemann[17)], C. Roda[2,14)], A. Rubbia[2,10)], F. Salvatore[13)], K. Schahmaneche[1)], B. Schmidt[2,17)], T. Schmidt[17)], M.E. Sevior[20)], D. Sillou[5)], F.J.P. Soler[2,8)], G. Sozzi[6)], D. Steele[6,7)], U. Stiegler[2)], M. Stipčević[21)], T. Stolarczyk[3)], M. Tareb-Reyes[6)], G.N. Taylor[20)], S. Tereshchenko[11)], A. Toropin[18)], A-M. Touchard[1)], S.N. Tovey[2,20)], M-T. Tran[6)], E. Tsesmelis[2)], J. Ulrichs[8)], L. Vacavant[6)], M. Valdata-Nappi[22,*)], V. Valuev[11,12)], F. Vannucci[1)], K.E. Varvell[8)], M. Veltri[16)], V. Vercesi[13)], J-M. Vieira[6)], T. Vinogradova[12)], F. Weber[2,9)], T. Weisse[17)], F.F. Wilson[2)], L.J. Winton[20)], B.D. Yabsley[8)], H. Zaccone[3)], K. Zuber[17)], and P. Zuccon[4)]

Abstract

The Λ polarization in ν_μ charged current interactions has been measured in the NOMAD experiment. The event sample (8087 reconstructed Λ's) is more than an order of magnitude larger than that of previous bubble chamber experiments, while the quality of event reconstruction is comparable. We observe negative polarization along the W-boson direction which is enhanced in the target fragmentation region: $P_x(x_F < 0) = -0.21 \pm 0.04(\text{stat}) \pm 0.02(\text{sys})$. In the current fragmentation region we find $P_x(x_F > 0) = -0.09 \pm 0.06(\text{stat}) \pm 0.03(\text{sys})$. These results provide a test of different models describing the nucleon spin composition and the spin transfer mechanisms. A significant transverse polarization (in the direction orthogonal to the Λ production plane) has been observed for the first time in a neutrino experiment: $P_y = -0.22 \pm 0.03(\text{stat}) \pm 0.01(\text{sys})$. The dependence of the absolute value of P_y on the Λ transverse momentum with respect to the hadronic jet direction is in qualitative agreement with the results from unpolarized hadron-hadron experiments.

(To be published in Nuclear Physics B)

[1] LPNHE, Univ. of Paris, Paris VI and VII, France.
[2] CERN, Geneva, Switzerland.
[3] DAPNIA, CEA Saclay, France.
[4] Univ. of Padova and INFN, Padova, Italy.
[5] LAPP, Annecy, France.
[6] University of Lausanne, Lausanne, Switzerland.
[7] Johns Hopkins Univ., Baltimore, MD, USA.
[8] Univ. of Sydney, Sydney, Australia.
[9] Harvard Univ., Cambridge, MA, USA.
[10] ETH Zürich, Zürich, Switzerland.
[11] JINR, Dubna, Russia.
[12] UCLA, Los Angeles, CA, USA.
[13] Univ. of Pavia and INFN, Pavia, Italy.
[14] Univ. of Pisa and INFN, Pisa, Italy.
[15] IFIC, Valencia, Spain.
[16] Univ. of Urbino, Urbino, and INFN Florence, Italy.
[17] Dortmund Univ., Dortmund, Germany.
[18] Inst. Nucl. Research, INR Moscow, Russia.
[19] Univ. of Florence and INFN, Florence, Italy.
[20] University of Melbourne, Melbourne, Australia.
[21] Rudjer Bošković Institute, Zagreb, Croatia.
[22] Univ. of Calabria and INFN, Cosenza, Italy.
[23] Univ. of South Carolina, Columbia, SC, USA.
[24] Roma-III Univ., Rome, Italy.
[*] Now at Univ. of Perugia and INFN, Perugia, Italy.

1 INTRODUCTION

1.1 The NOMAD experiment

The main goal of the NOMAD experiment [1] is the search for $\nu_\mu \to \nu_\tau$ oscillations in the wide-band neutrino beam from the CERN SPS. The main characteristics of the beam are given in Table 1. This search uses kinematic criteria to identify ν_τ charged current (CC) interactions [2] and requires a very good quality of event reconstruction similar to that of bubble chamber experiments. This has indeed been achieved by the NOMAD detector, and, moreover, the large data sample collected during four years of data taking (1995-1998) allows for a detailed study of neutrino interactions. The data are compared to the results of a Monte Carlo (MC) simulation based on LEPTO 6.1 [3] and JETSET 7.4 [4] generators for neutrino interactions and on a GEANT [5] based program for the detector response.

Table 1: The CERN SPS neutrino beam composition (as predicted by the beam simulation program).

Neutrino	Flux		CC interactions in NOMAD	
flavours	$< E_\nu >$ [GeV]	rel.abund.	$< E_\nu >$ [GeV]	rel.abund.
ν_μ	23.5	1	43.8	1
$\bar{\nu}_\mu$	19.2	0.0612	42.8	0.0255
ν_e	37.1	0.0094	58.3	0.0148
$\bar{\nu}_e$	31.3	0.0024	54.5	0.0016

An analysis of the full data sample (corresponding to 1.3×10^6 ν_μ CC interactions) devoted to the study of the Λ *hyperon polarization* in neutrino deep inelastic scattering (DIS) is presented in this article. This study relies on an efficient and robust Λ hyperon identification algorithm. Λ hyperons are identified via their decays $\Lambda \to \mathrm{p}\pi^-$ which appear in the detector as two charged tracks with opposite charges emerging from a common vertex separated from the primary interaction vertex (V^0-like signature).

The Λ polarization is measured by the *asymmetry* in the angular distribution of the protons in the parity violating decay process $\Lambda \to \mathrm{p}\pi^-$. In the Λ rest frame the decay protons are distributed as:

$$\frac{1}{N}\frac{\mathrm{d}N}{\mathrm{d}\Omega} = \frac{1}{4\pi}(1 + \alpha_\Lambda \mathbf{P} \cdot \mathbf{k}), \tag{1}$$

where $\mathbf{P}$ is the Λ polarization vector, $\alpha_\Lambda = 0.642 \pm 0.013$ [8] is the decay asymmetry parameter and $\mathbf{k}$ is the unit vector along the decay proton direction.

For the Λ polarization measurement the tracking capabilities of a detector are of paramount importance. The NOMAD detector (see Fig. 1) is especially well suited to this aim. It consists of an active target of 44 drift chambers, with a total fiducial mass of 2.7 tons, located in a 0.4 Tesla dipole magnetic field. The drift chambers [6], made of low Z material (mainly Carbon) serve the double role of a (nearly isoscalar) target for neutrino interactions and of the tracking medium. The average density of the drift chamber volume is 0.1 g/cm^3. These drift chambers provide an overall efficiency for charged track reconstruction of better than 95% and a momentum resolution of approximately 3.5% in the momentum range of interest (less than 10 GeV/c). Reconstructed tracks are used to determine the event topology (the assignment of tracks to vertices), to reconstruct the vertex position and the track parameters at each vertex and, finally, to identify the vertex type (primary, secondary, V^0, etc.). A lead-glass electromagnetic calorimeter [7] located

downstream of the tracking region provides an energy resolution of $3.2\%/\sqrt{E[\mathrm{GeV}]} \oplus 1\%$ for electromagnetic showers and is essential to measure the total energy flow in neutrino interactions. In addition, an iron absorber and a set of muon chambers located after the electromagnetic calorimeter are used for muon identification, providing a muon detection efficiency of 97% for momenta greater than 5 GeV/c.

The *large statistics of these data* combined with the *good quality of event reconstruction* in the NOMAD detector allows a detailed study of the Λ polarization as a function of different kinematic variables.

The article is organized as follows. Subsection 1.2 gives a theoretical introduction, while in subsection 1.3 the current experimental situation is reviewed. In section 2 we describe the method and final results of the V^0 identification procedure. The polarization analysis is described in section 3. Results are presented in section 4, while section 5 gives our estimate of systematic errors from different sources. Finally, section 6 is devoted to a summary and conclusions.

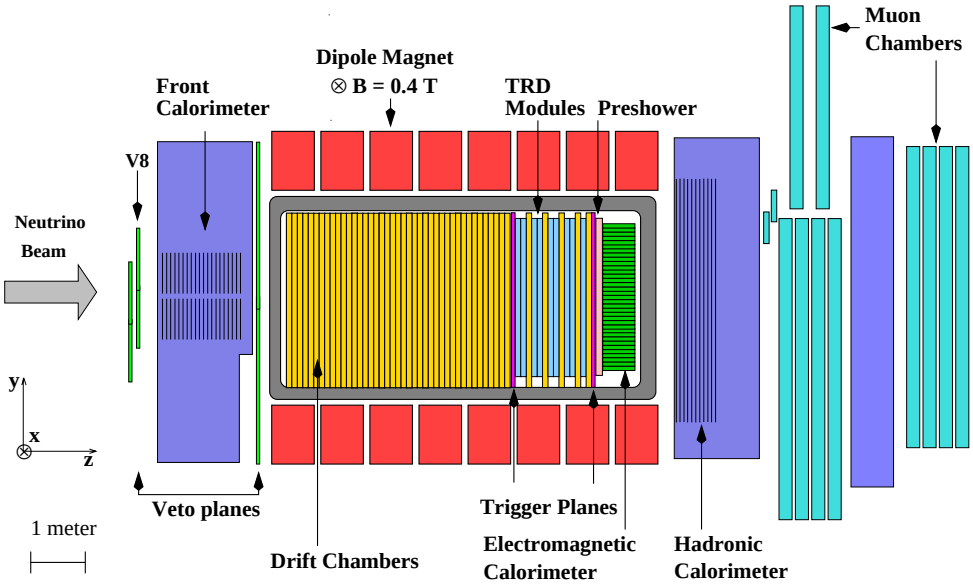

Figure 1: A sideview of the NOMAD detector.

1.2 Theoretical considerations

Renewed interest in spin phenomena in high energy physics has arisen after the European Muon Collaboration (EMC) discovered [9], and later the Spin Muon Collaboration (SMC) confirmed [10], that the quark contribution to the proton spin

$$\Sigma = \Delta u + \Delta d + \Delta s = 0.27 \pm 0.04, \quad \text{at } Q^2 = 10 \text{ GeV}^2 \tag{2}$$

(where Δq is the polarized quark structure function in the nucleon) is substantially smaller than expected. Theoretical expectations vary from $\Sigma = 1$ in the static quark model to $\Sigma \approx 0.6$, where the last value is based on experimental measurements of axial matrix elements in hyperon β decays under the assumption of negligible contribution from strange quarks.

If in addition exact $SU(3)$ flavour symmetry is assumed, then the SMC results in Eq. 2 combined with measurements of hyperon β decays provide an estimate of the different quark contributions to the nucleon spin, under the assumption of zero contribution from gluons:

$$\Delta u = 0.82 \pm 0.03, \quad \Delta d = -0.44 \pm 0.03, \quad \Delta s = -0.11 \pm 0.03 \tag{3}$$

This result indicates a non-negligible contribution from strange sea quarks, though the interpretation strongly depends on the gluon part of the nucleon spin. The gluon U(1) anomaly can be a source of a non-zero gluon contribution ΔG to the nucleon spin [11]. It suggests that every polarized quark structure function Δq should be corrected as $\Delta q \longrightarrow \Delta q - \frac{\alpha_s}{2\pi}\Delta G$.

Today it is believed that the nucleon spin is distributed among quarks (valence and sea), gluons, and their orbital momenta (L_q and L_g for quarks and gluons respectively) [12]:

$$S_z = \frac{1}{2}\Sigma + L_q + \Delta G + L_g = \frac{1}{2} \tag{4}$$

It is possible that both gluons and sea quarks contribute significantly to the nucleon spin. There are dedicated experiments, e.g. E143 [13] at SLAC and HERMES [14] at DESY, investigating the nucleon spin content via deep inelastic scattering of longitudinally polarized electrons (positrons) from polarized targets.

However, some important questions are still challenging theoretical and experimental investigations, namely:

- what is the origin of the gluon polarization inside the nucleon?
- are strange quarks polarized inside the nucleon?
- what is the spin content of other baryons?

Polarized lepton nucleon DIS with a Λ hyperon in the final state can shed light on the last two questions. Λ hyperons are unique among baryons due to their relatively large production rate and because of their parity violating weak decay $\Lambda \rightarrow p\pi^-$. Different physical mechanisms are responsible for the Λ polarization in different x_F regions ($x_F = 2p_L^*/W$). In the target fragmentation region ($x_F < 0$) the origin of the Λ polarization could be either polarized strange quarks from the target nucleon, or the polarization transfer from the polarized di-quark which is left behind after the lepton nucleon DIS, or both. In the current fragmentation region ($x_F > 0$) the polarized struck quark transfers its polarization to the Λ hyperon. Since a large fraction of Λ's is produced via the decays of heavier baryons and resonances, this effect should be taken into account in any theoretical attempt to explain the Λ polarization results. Below we consider in more detail the different theoretical approaches suggested to explain the Λ polarization in the target and current fragmentation regions.

1.2.1 Target fragmentation region

The polarized intrinsic strange content of the nucleon can be tested via polarization measurements of Λ hyperons produced in lepton-nucleon DIS by the asymmetry in the angular distribution of protons in the parity violating $\Lambda \rightarrow p\pi^-$ decay (see Eq. 1). The authors of Refs. [15, 16] advocate a model with negatively polarized intrinsic sea $s\bar{s}$ pairs in the nucleon. This model is based on two observations:

- the pseudo-scalar mesons, like π's, K's and η's, are light on the typical hadronic mass scale. This can be interpreted as the reflection of a strong effective quark-antiquark attraction in the $J^P = 0^-$ state.

- the density of quark-antiquark pairs in the non-perturbative vacuum is quite high [17]:

$$< 0|\bar{u}u|0 > \approx < 0|\bar{d}d|0 > \approx (250 \text{ MeV})^3, \quad < 0|\bar{s}s|0 > \approx (0.8 \pm 0.1) < 0|\bar{q}q|0 >,$$

where $q = u, d$.

As originally stated in Refs. [15, 16] the polarization of the $s\bar{s}$ pair is anticorrelated to the spin of the *target nucleon*, thus the model predicts opposite signs for the longitudinal Λ polarization in νn (negative) and νp (positive) DIS. On the other hand it is possible to reformulate this model in such a way that the polarization of the $s\bar{s}$pair is anticorrelated to the spin of the *struck quark*. In this case the model [15, 16] predicts negative longitudinal polarization in both νn and νp DIS (as shown in Fig. 2). Thus, measurements of the longitudinal Λ polarization in (anti)neutrino DIS on both neutron and proton targets could resolve this ambiguity.

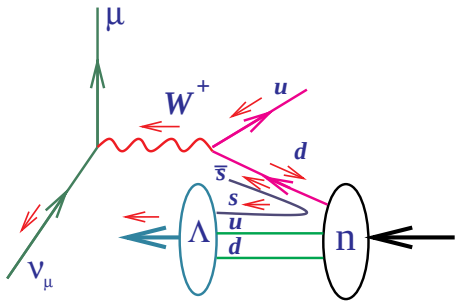

Figure 2: Dominant diagram for Λ production in the target fragmentation region due to scattering on a valence d quark in a neutron.

Negatively polarized intrinsic sea $s\bar{s}$ pairs in the nucleon can manifest themselves in a *negative longitudinal* polarization of Λ hyperons produced in (anti)neutrino-nucleon DIS in the target fragmentation region (see Fig. 2). Any quantitative prediction in the framework of this model depends strongly on the spin correlation function between the struck quark and the $s\bar{s}$ pair as well as on the quark spin content of the Λ hyperon.

As first pointed out by Bigi [18], the remnant di-quark which is left behind during polarized lepton-nucleon DIS can also be polarized and can transfer its polarization to a baryon (Σ^0, Ξ, $\Sigma^\star$) which in turn can transfer its polarization to a Λ hyperon into which it decays. Therefore a theoretical interpretation of the Λ polarization measurements in the target fragmentation region relies on the baryon spin content as well as on the relative production rates of each species.

1.2.2 Current fragmentation region

There exist two different schemes for the baryon spin content. According to the static quark model, the spin of a baryon belonging to the $J^P = \frac{1}{2}^+$ octet is determined by the three valence quarks, while polarized lepton-nucleon scattering data and $SU(3)$ flavour symmetry in hyperon decay imply that the total spin carried by the valence quarks is only part of the spin of a baryon. The measurement of the Λ polarization is an ideal tool to test different spin transfer mechanisms. In the static quark model the Λ spin is determined by the strange quark only. DIS data together with $SU(3)$ flavour symmetry in hyperon decay suggest that the s quark carries only about 60% of the Λ spin, while u and d quarks contribute about -20% each (the BJ model [19]). An experiment with a source of polarized quarks could determine which of these two schemes is effective in nature.

However, in a given experimental setup Λ's produced directly are often indistinguishable from those which are decay products of heavier hyperons. These hyperons can also be polarized and transfer their polarization to Λ's in the decay processes. The static quark model which takes into account polarization transfer from other hyperons is known as the BGH model [18, 20].

There are several possibilities to measure the polarized fragmentation functions in different processes. One promising method from a theoretical point of view is based on the measurement of the polarization of Λ's produced in e^+e^- annihilation at the Z^0 pole. Unfortunately existing data provide only a poor constraint to the models (see [21, 22, 23, 24, 25]).

Measurements of the longitudinal (along the current direction) Λ polarization in charged lepton nucleon DIS have also been analyzed and discussed [26]. Under the assumption of u quark dominance in charged lepton-nucleon DIS it is possible to extract the spin transfer coefficient $C_u^\Lambda = \Delta D_u^\Lambda(z)/D_u^\Lambda(z)$, where $D_u^\Lambda(z)$ and $\Delta D_u^\Lambda(z)$ are the unpolarized and polarized fragmentation functions respectively (here and in what follows x_B and y_B are the standard Bjorken variables describing the DIS process and z is the fraction of the total hadronic energy carried away by the Λ in the laboratory frame):

$$P_\Lambda \approx P_B D(y_B) \frac{\Delta D_u^\Lambda(z)}{D_u^\Lambda(z)} = P_B D(y_B) C_u^\Lambda, \tag{5}$$

where P_B is the beam polarization, and $D(y_B)$ is the longitudinal depolarization factor of a virtual photon. Such processes are under study both theoretically (see e.g. Ref. [23]) and experimentally at HERMES [27], E665 [28] and the forthcoming COMPASS project [29]. However, because of the typical factor $P_B D(y_B) \approx 0.3$ statistical errors in the measurements of P_Λ will translate into errors on C_u^Λ which are larger by a factor of three. Current data are still not precise enough to draw final conclusions on the spin transfer mechanism.

Among other sources of polarized beams, neutrinos and antineutrinos can play an exceptional role. The (anti)neutrino in deep inelastic scattering from a nucleon interacts with a *polarized quark of specific flavour* in the nucleon (see Fig. 3), and this particular property makes (anti)neutrino DIS processes an ideal experimental tool to study flavour dependent quark fragmentation functions, testing different spin transfer mechanisms. The polarization of directly produced Λ's in $\nu_\mu N \to \mu^- \Lambda X$ is determined by the following expression:

$$P_\Lambda(x_B, y_B, z) = -\frac{d(x_B)\Delta D_u^\Lambda(z) - (1-y_B)^2 \bar{u}(x_B)\Delta D_{\bar{d}}^\Lambda(z)}{d(x_B) D_u^\Lambda(z) + (1-y_B)^2 \bar{u}(x_B) D_{\bar{d}}^\Lambda(z)}, \tag{6}$$

where for the sake of simplicity the Cabibbo suppressed processes and the contribution from strange quarks inside the target are neglected. It is easy to see from Eq. 6 that due to the smaller contribution from the $\bar{u}$ quark, and due to the suppression factor $(1-y_B)^2$, a measurement of the Λ polarization in $\nu_\mu N \to \mu^- \Lambda X$ DIS provides a measurement of C_u^Λ with *the same statistical error* as the one affecting the Λ polarization itself. In an experiment with sufficient statistics of Λ and $\bar{\Lambda}$ in ν_μ CC and in $\bar{\nu}_\mu$ CC, it is possible to provide a clean separation of unpolarized and polarized fragmentation functions of a quark into Λ and $\bar{\Lambda}$ for both light-flavour and strange (anti)quarks [30, 31].

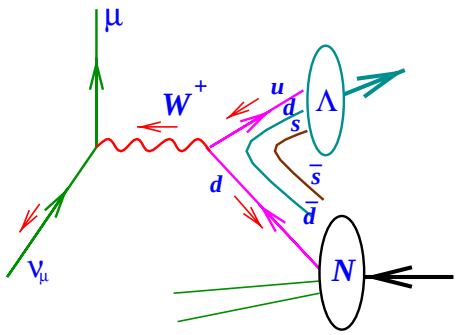

Figure 3: Dominant diagram for Λ production in the current fragmentation region due to scattering on a valence d quark.

1.3 Review of experimental data

Several neutrino experiments have reported measurements of the Λ polarization [32, 33, 34, 35, 36] but the experimental situation in this field is still confused.

A negative *longitudinal* polarization of Λ's with respect to the W-boson direction has been observed in several (anti)neutrino experiments, while the absolute value of the polarization varied over a wide range from 0.1 to 0.56 with a statistical error in the range $0.13 \div 0.17$ (see P_x component in Table 2). The effect is enhanced in the target fragmentation region ($x_F < 0$). Estimates of the systematic uncertainties on these results vary in different studies from 0.02 up to the size of the statistical errors. According to the authors, the largest contribution to the systematic bias comes from the K^0_s induced background.

Table 2: The Λ polarization measured in previous neutrino experiments. The results are given in the "J" system, with the axes defined in the Λ rest frame as follows: $\mathbf{n}_x = \vec{e}_W$, $\mathbf{n}_y = \frac{\vec{e}_W \times \vec{e}_T}{|\vec{e}_W \times \vec{e}_T|}$, $\mathbf{n}_z = \mathbf{n}_x \times \mathbf{n}_y$, where $\vec{e}_W$ is a unit vector in the current (W boson) direction and $\vec{e}_T$ is a unit vector in the direction of the target nucleon (assumed to be initially at rest in the laboratory). $< E_\nu >$ is the average (anti)neutrino energy of the charged current event sample.

Reaction Experiment	$< E_\nu >$ [GeV]	Selection	N_Λ	P_x	P_y	P_z
$\nu_\mu - p$	51	Full sample	289	-0.10 ± 0.14	-0.02 ± 0.16	0.12 ± 0.15
WA21 [32]		$x_F < 0$	203	-0.29 ± 0.18	-0.09 ± 0.19	0.19 ± 0.18
		$x_F > 0$	86	0.53 ± 0.30	0.08 ± 0.28	0.04 ± 0.29
$\bar{\nu}_\mu - p$	40	Full sample	267	-0.24 ± 0.17	-0.05 ± 0.16	-0.20 ± 0.17
WA21 [32]		$x_F < 0$	210	-0.38 ± 0.18	0.02 ± 0.18	-0.17 ± 0.18
		$x_F > 0$	57	0.32 ± 0.35	-0.38 ± 0.34	-0.30 ± 0.36
$\bar{\nu}_\mu - Ne$	40	Full sample	469	-0.56 ± 0.13	-0.02 ± 0.13	0.08 ± 0.13
WA59 [33]		$x_F < 0$	403	-0.63 ± 0.13	-0.02 ± 0.14	0.12 ± 0.14
		$x_F > 0$	66	-0.11 ± 0.45	-0.06 ± 0.40	-0.01 ± 0.44
$\nu_\mu - Ne$	150	Full sample	258	-0.38 ± 0.16	-0.04 ± 0.17	-0.17 ± 0.18
E632 [34]		$x_F < 0$	190	-0.43 ± 0.20	-0.06 ± 0.19	-0.45 ± 0.19

The *transverse* (orthogonal to the production plane) polarization of Λ hyperons produced in (anti)neutrino - nucleon interactions has also been studied. Two early antineutrino experiments [35, 36] have reported, within large errors, indications of a transverse Λ polarization (with opposite signs in different experiments: see P_N component in

Table 3). These results have not been confirmed by later measurements (see P_y component in Table 2).

Table 3: The transverse Λ polarization measured in previous neutrino experiments. The results are given in the reference system in which the axes are defined as follows: $\mathbf{n}_L = \vec{e}_\Lambda$, $\mathbf{n}_N = \frac{\vec{e}_\Lambda \times \vec{e}_\nu}{|\vec{e}_\Lambda \times \vec{e}_\nu|}$, $\mathbf{n}_T = \mathbf{n}_N \times \mathbf{n}_L$, where $\vec{e}_\nu$ is a unit vector in the incoming (anti)neutrino direction and $\vec{e}_\Lambda$ is a unit vector in the direction of motion of the Λ hyperon. $< E_\nu >$ is the average (anti)neutrino energy of the charged current event sample.

Reaction Experiment	$< E_\nu >$ [GeV]	Selection	N_Λ	P_L	P_T	P_N
$\bar{\nu}_\mu - Ne$						
E180 [35]	43	Full sample	187	-0.15 ± 0.20	-0.12 ± 0.19	0.34 ± 0.18
$\bar{\nu}_\mu - d$	43	Full sample	181	–	–	-0.32 ± 0.20
WA25 [36]		$x_B < 0.3$	136	–	–	-0.57 ± 0.22
$\nu_\mu - d$	55	Full sample	234	–	–	0.06 ± 0.18
WA25 [36]		$x_B < 0.3$	166	–	–	-0.06 ± 0.21

We point out that all the previous measurements of the Λ polarization in (anti)neutrino experiments performed with bubble chambers suffered from the *low statistics* of the Λ samples.

The NOMAD experiment can study the Λ polarization in both target fragmentation and current fragmentation regions simultaneously, thus achieving two goals: looking for the polarization of the intrinsic strange component of the nucleon and measuring polarized fragmentation functions in $\nu_\mu N \to \mu^- \Lambda X$ as well as in $\nu_\mu N \to \mu^- \bar{\Lambda} X$ and $\bar{\nu}_\mu N \to \mu^+ \Lambda X$ (both statistically limited).

This paper is limited to the measurement of the Λ polarization in ν_μ CC DIS. The NOMAD data provide more than an order of magnitude increase in statistics, thus allowing a detailed study of both longitudinal and transverse Λ polarizations as a function of different kinematic variables.

2 EVENT SELECTION AND V^0 IDENTIFICATION PROCEDURE

The first step in the polarization analysis consists of building a robust and efficient neutral strange particle identification procedure. To minimize the statistical errors and to eliminate any background-related systematic bias, our identification procedure should optimize both the selection efficiency and the purity of the final Λ sample. Special efforts are needed to suppress as much as possible γ-related background (photon conversions) and contamination from other neutral strange particle decays. Moreover, the event kinematics of the neutrino interaction must be properly reconstructed.

2.1 Selection of ν_μ CC events

The following *quality cuts* are imposed to select a clean sample of ν_μ CC interactions both in data and Monte Carlo events:

- presence of an identified muon at the primary vertex;
- both primary and V^0 vertices in the fiducial volume:
  $|X, Y| < 120$ cm, 5 cm $< Z <$ 395 cm;
- reconstructed neutrino energy $E_\nu < 450$ GeV.

For the incoming neutrino energy calculation we use the total visible energy defined as:

$$E_\nu = E_\mu + \sum E_c + \sum E_n,$$

where E_μ is the energy of the identified muon, $\sum E_c$ is the sum of the energy of reconstructed charged tracks (assuming the mass of the pion if the particle type is not explicitly identified) and $\sum E_n$ contains identified decays of neutral particles, photon conversions, secondary vertices corresponding to interactions of neutral particles and the energy of photons measured by the electromagnetic calorimeter.

2.2 V^0 selection

The decays $\mathrm{K}^0_\mathrm{s} \to \pi^+\pi^-$, $\Lambda \to p\pi^-$, $\bar{\Lambda} \to \bar{p}\pi^+$ and photon conversions $\gamma \to e^+e^-$ appear in the detector as V^0 type vertices: two charged tracks with opposite charges emerging from a common vertex separated from the primary neutrino interaction vertex (see Fig. 4 as an example).

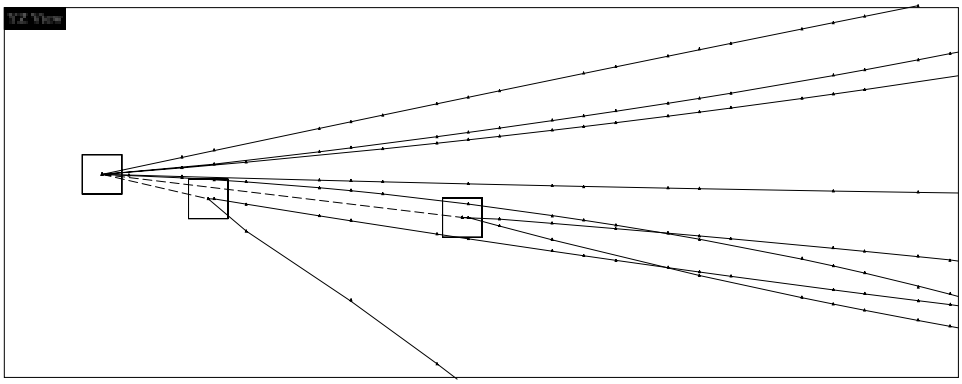

Figure 4: A reconstructed data event containing 2 V^0 vertices identified as Λ and $\bar{\Lambda}$ decays by the identification procedure (see below). The scale on this plot is given by the size of the vertex boxes (3×3 cm^2).

The following *selection criteria* have been applied to the reconstructed V^0 candidates:

- χ^2 probability of the V^0 vertex reconstruction larger than 0.01;
- transverse component p_T^{dirv} of the total momentum of the two outgoing charged tracks with respect to the line connecting the primary and V^0 vertices smaller than 100 MeV/c. This cut rejects V^0's with momentum not pointing to the primary vertex and also V^0's which do not come from two-body decays (e.g. neutron interactions).
- transverse component p_T^{int} of the momentum of one of the outgoing charged tracks with respect to the V^0 momentum greater than 20 MeV/c. This cut is crucial to eliminate a large fraction of photon conversions.
- measured proper decay time τ consistent with the tested hypothesis $\tau < 6\ \tau_{V^0}(\mathrm{PDG})$, where $\tau_{V^0}(\mathrm{PDG})$ is the lifetime as given in Ref. [8].

2.3 Neutral strange particle identification

Since the NOMAD detector is unable to distinguish protons from pions in the momentum range relevant to this analysis, any V^0 identification procedure should rely on

the kinematic properties of a V^0 decay:

- the positive and negative track momenta ($p^{\pm}$) and related kinematic variables shown in Fig. 5, e.g. p_T^{int}, and the longitudinal momentum asymmetry between the positive and negative tracks, $\alpha = (p_L^+ - p_L^-)/(p_L^+ + p_L^-)$;
- invariant mass, proper decay time, etc. calculated with the appropriate mass assignment of the outgoing particles for the given decaying parent (Λ, K_s^0, $\bar{\Lambda}$).

The study of different V^0 hypotheses based on the distributions of kinematic variables leads to *identified* V^0's of two types:

- *uniquely* identified V^0's which populate kinematic regions corresponding to different values of the discriminating variables;
- *ambiguously* identified V^0's due to overlapping kinematic regions from the decay of different particles

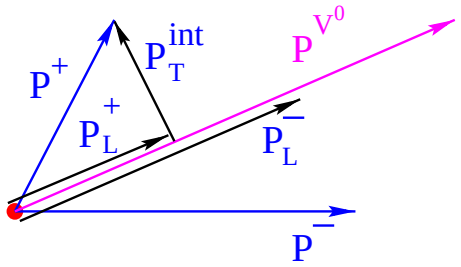

Figure 5: Schematic definition of kinematic variables used for the neutral strange particle identification.

Wrong assignments of events and inadequate evaluation of background would lead to systematic errors in the measurement of the Λ polarization. Additional sources of systematic errors could come from an incorrect MC simulation of the relative V^0 yields. It is therefore clear that any identification procedure based on kinematic selections should minimize such effects and allow an evaluation of the systematic errors associated to them.

Two different methods of V^0 identification using kinematic variables have been developed.

The first method is based on a preliminary selection of uniquely identified V^0's and on a treatment of the ambiguous ones (passing the cuts for two hypotheses) by the use of the likelihood ratios which take into account the correlations between the discriminant variables chosen for this analysis [37].

The second method of V^0 identification is based on a kinematic fit with energy and momentum conservation constraints (details of the kinematic fit can be found in [38, 39, 40, 41]). This fit has been performed for three decay hypotheses: $\mathrm{K}_\mathrm{s}^0 \to \pi^+\pi^-$, $\Lambda \to p\pi^-$, $\bar{\Lambda} \to \bar{p}\pi^+$ and for the hypothesis of a photon conversion $\gamma \to e^+e^-$ [42]. The treatment of ambiguities is motivated by the need of selecting the corresponding V^0 decays with highest efficiency and lowest background contamination from other V^0 types. The output of the kinematic fits applied to a given V^0 vertex consists of four $\chi^2_{V^0}$. Using these variables the corresponding regions in the four-dimensional $\chi^2_{V^0}$ space populated by particles identified as Λ's, K_s^0's, and $\bar{\Lambda}$'s have been selected. These regions can be subdivided into uniquely and ambiguously identified subsamples. The ambiguous part of the identified sample adds more statistics but with a significant background contamination. The latter must be well under control in case of possible differences between data and MC predictions. An optimum compromise between high statistics of the identified V^0 sample and

well understood background contamination is the aim of our identification strategy which consists of two steps:

1) we select a subsample of uniquely identified V^0's with high purity (98% for K^0_s's, 97% for Λ's, 90% for $\bar{\Lambda}$'s) requiring the fraction of the uniquely identified V^0's in the final sample to be more than 90%;
2) then we add a subsample of ambiguously identified V^0's resolving the ambiguities between Λ/K^0_s and $\bar{\Lambda}/K^0_s$ in favour of maximal efficiency and maximal purity of each V^0 category.

To illustrate the quality of the identification procedure Fig. 6 shows reconstructed invariant mass distributions for identified Λ's and K^0_s's.

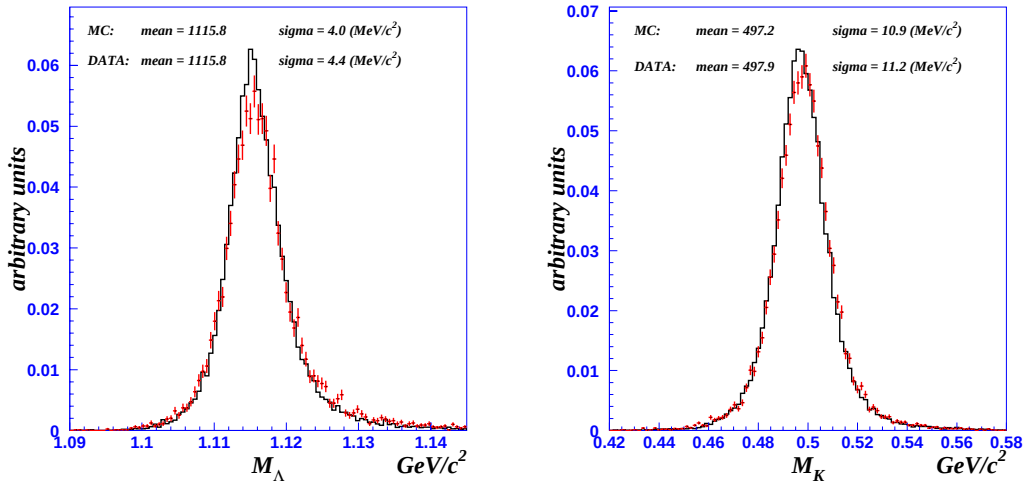

Figure 6: Normalized invariant mass distribution for identified Λ (left) and K^0_s (right): comparison of data (points with error bars) and MC simulation (histogram).

Figure 7 shows the $p_T^{\rm int}$ vs α plot before and after application of the V^0 selection and identification procedures. Three regions corresponding to $K^0_s \to \pi^+\pi^-$, $\Lambda \to p\pi^-$ and $\bar{\Lambda} \to \bar{p}\pi^+$ decays are clearly visible. From this plot one can conclude that the main background for the Λ and $\bar{\Lambda}$ identification is due to K^0_s's in both methods.

The identification procedures described above have the common feature of producing a distortion in the decay phase space of identified Λ's (see Fig. 8, left). This effect is well reproduced by comparing data and reconstructed Monte Carlo events. The distortion is due to the method adopted to maximize the purity of the Λ sample.

In addition, an original identification method (the α-asymmetry method, described in [37]) has been developed. The K^0_s sample is expected to be symmetric with respect to the parameter α, while the Λ and $\bar{\Lambda}$ samples are expected to be strongly asymmetric. This can be seen in Fig. 7, where 5 different boxes are defined. The exact symmetry for K^0_s is proven by subtracting box III from box IV (which are both populated by K^0_s only). Subtracting box I from box II, the K^0_s component is exactly compensated. Λ's populate only box II. They are about 10 times more abundant than $\bar{\Lambda}$'s, which populate only box I. Thus, the subtraction procedure extracts a sample of events representing about 90% of the original sample with the kinematic properties of a pure Λ sample. This approach is free from the problem of distortion in the decay phase space (see Fig. 8, right). In this method the background is mainly due to $\bar{\Lambda}$'s, rather than K^0_s's as in the case of the kinematic

fit approach. This technique can be safely applied to the region of $x_F < 0$ since $\bar{\Lambda}$'s are mainly produced in the current fragmentation region. For these reasons the α-asymmetry method, which gives results similar to the ones obtained with the kinematic fit selection, adds confidence in the final measurement of the Λ polarization. However, this method cannot be used for V^0 identification on an event by event basis.

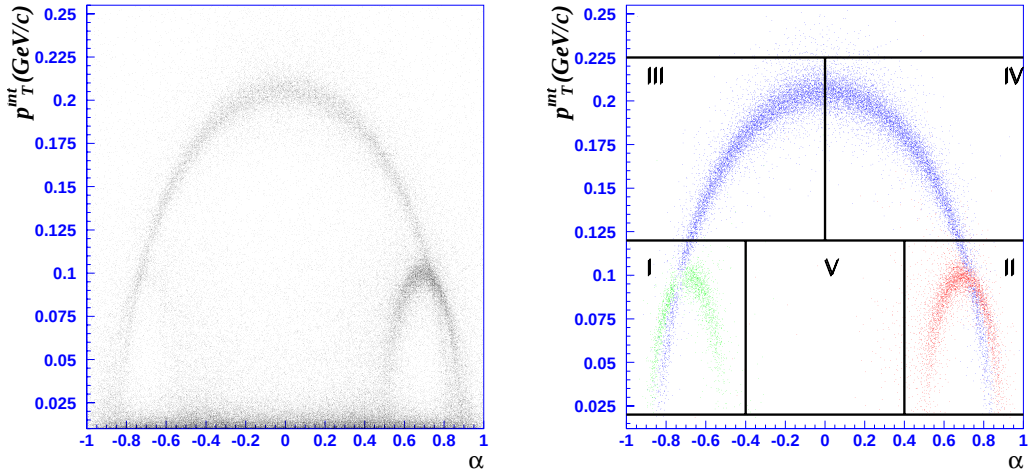

Figure 7: $p_T^{\rm int}$ vs α plot for V^0's in data events before (left) and after (right) the V^0 selection and identification procedures. $\bar{\Lambda}$'s and Λ's populate boxes I and II respectively. The K^0_s sample being symmetric is the content of all the other boxes except box V. Photon conversions populate the small $p_T^{\rm int}$ region.

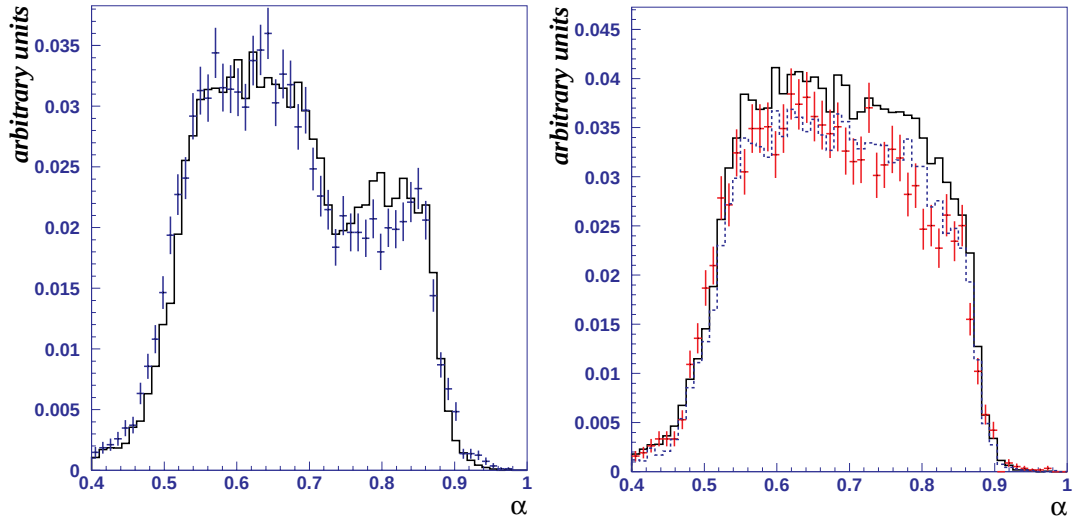

Figure 8: Normalized distributions of α for Λ's identified with the help of the kinematic fit selection (left) and the α-asymmetry method (right). Both simulated events (histogram) and data (points with error bars) are shown. The plot corresponding to the α-asymmetry method shows reconstructed true Λ's in simulated events (solid line) and Λ's identified by the α-asymmetry method both in MC (dashed line) and data (points with error bars).

Similar results have been obtained using all these approaches with respect to both the quality of the neutral strange particle selection and the polarization measurements. The kinematic fit method is used in the analysis presented here.

2.4 V^0 identification results

We define reconstruction (ϵ_r), selection (ϵ_s) and identification (ϵ_i) efficiencies for simulated V^0's in the following way:

$$\begin{aligned} \epsilon_r &= \frac{\text{Number of reconstructed } \ V^0 \to h^+h^- \text{ decays}}{\text{Number of simulated } \ V^0 \to h^+h^- \text{ decays}} \\ \epsilon_s &= \frac{\text{Number of selected } \ V^0 \to h^+h^- \text{ decays}}{\text{Number of reconstructed } \ V^0 \to h^+h^- \text{ decays}} \\ \epsilon_i &= \frac{\text{Number of identified } \ V^0 \to h^+h^- \text{ decays of the correct type}}{\text{Number of selected } \ V^0 \to h^+h^- \text{ decays}} \end{aligned} \tag{7}$$

These efficiencies are calculated using a large sample of ν_μ CC MC interactions in the detector fiducial volume.

The reconstruction efficiency reflects the quality of the NOMAD detector and of the corresponding reconstruction algorithms, while the identification efficiency shows our capability to identify a preselected neutral strange particle decay. The global efficiency (ϵ) is given by: $\epsilon = \epsilon_r \times \epsilon_s \times \epsilon_i$. The purity for a given sample is defined as:

$$P = \frac{\text{Number of identified } \ V^0 \to h^+h^- \text{ decays of the correct type}}{\text{Number of identified } \ V^0 \to h^+h^- \text{ decays}} \tag{8}$$

Results are summarized in Table 4 which also gives the number of neutral strange particles selected in the data by our identification procedure.

Table 4: Efficiencies (reconstruction, selection, identification, global) and purity of each selected V^0 sample (see text for details). Numbers of identified neutral strange particles in the data are also shown in the last column.

V^0	ϵ_r (%)	ϵ_s (%)	ϵ_i (%)	ϵ (%)	P (%)	Data
K^0_s	30.7	78.8	91.3	22.1 ± 0.1	97.2 ± 0.1	15074
Λ	24.8	79.0	83.4	16.4 ± 0.1	95.9 ± 0.1	8087
$\bar{\Lambda}$	37.5	76.3	65.2	18.6 ± 0.5	89.7 ± 0.7	649

From Table 4 one can conclude that the number of identified neutral strange particles in the NOMAD experiment is $\sim$ 20 times larger than in any previous neutrino experiment which has reported a measurement of the Λ polarization (see Tables 2 and 3). The global efficiency is $\simeq$ 20% while the purity is quite high: the final Λ sample consists of 95.9% true Λ's, 2.3% misidentified K^0_s's, 0.2% misidentified γ's and 1.6% other backgrounds including random track associations.

3 POLARIZATION ANALYSIS

3.1 Reference system

Having identified Λ's produced in ν_μ CC DIS one can try to extract their preferential spin orientation with respect to the physical vectors of the event. One may choose one of the following unit vectors: exchanged W-boson direction ($\vec{e}_W$), direction of the

target nucleon ($\vec{e}_T$), incoming neutrino direction ($\vec{e}_\nu$), and the vector orthogonal to the production plane (defined below). There is some freedom in choosing the corresponding coordinate system, where the x-axis can be a unit vector along $\vec{e}_W$, $\vec{e}_T$ or $\vec{e}_\nu$. These frames are known as "J", "T", and "ν" coordinate systems respectively and self consistent measurements of the polarization vector can be made in all these systems (see Section 5). For the polarization analysis described below we use the "J" reference system, where axes are defined as follows (in the Λ rest frame):

- the $\mathbf{n}_x$ axis is chosen along the reconstructed W-boson direction ($\vec{e}_W$);
- the $\mathbf{n}_y$ axis is orthogonal to the Λ production plane (defined as the plane containing both the target nucleon and the W-boson vectors):
  $\mathbf{n}_y = \vec{e}_W \times \vec{e}_T / |\vec{e}_W \times \vec{e}_T|$.
- the $\mathbf{n}_z$ axis is chosen to form a right-handed coordinate system:
  $\mathbf{n}_z = \mathbf{n}_x \times \mathbf{n}_y$.

The correct determination of the W-boson 4-vector is crucial for the definition of the "J" reference system. To compute the W-boson 4-vector we have used the well-defined muon information:

$$p_X^W = -p_X^\mu, \quad p_Y^W = -p_Y^\mu, \quad p_Z^W = E_\nu - p_Z^\mu, \quad E_W = E_\nu - E_\mu,$$

where Z axis is along the neutrino beam direction and the major uncertainty is due to the incoming neutrino energy estimated as described in Section 2.1.

Moreover, it is important to demonstrate the ability of our detector to reconstruct correctly the direction of the outgoing decay proton in the "J" reference system defined above. Figure 9 shows obvious correlations between reconstructed and simulated angular variables $\cos\theta_i = \mathbf{n}_i \cdot \mathbf{k}$, where $\mathbf{k}$ is the unit vector in the direction of the decay proton.

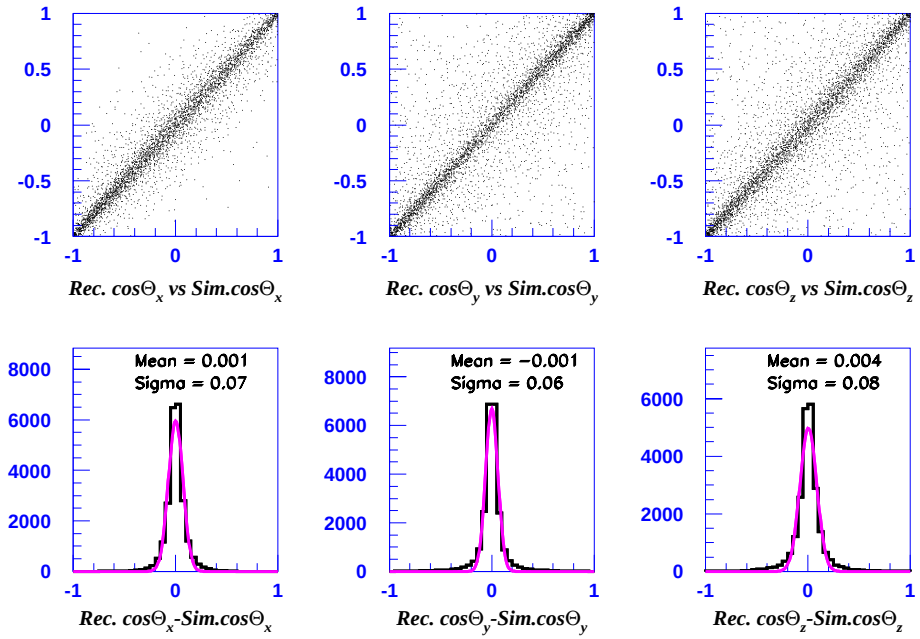

Figure 9: Correlations between generated and reconstructed angular variables for identified Λ's in ν_μ CC MC events.

A fit of the raw angular distributions of the decay protons in the data can only be performed after correction for detector acceptance. One of the most important contributions to the Λ reconstruction inefficiency comes from the loss of low energy pions

(see Fig. 10). If this effect is not properly accounted for, it could induce a fake asymmetry in the angular distributions and thus cause a fake "polarization". The full MC simulation of neutrino interactions in the NOMAD detector has been used to take this effect into account and to compute the Λ reconstruction and identification efficiencies (see Section 2.4).

In our MC simulation Λ hyperons are not polarized.

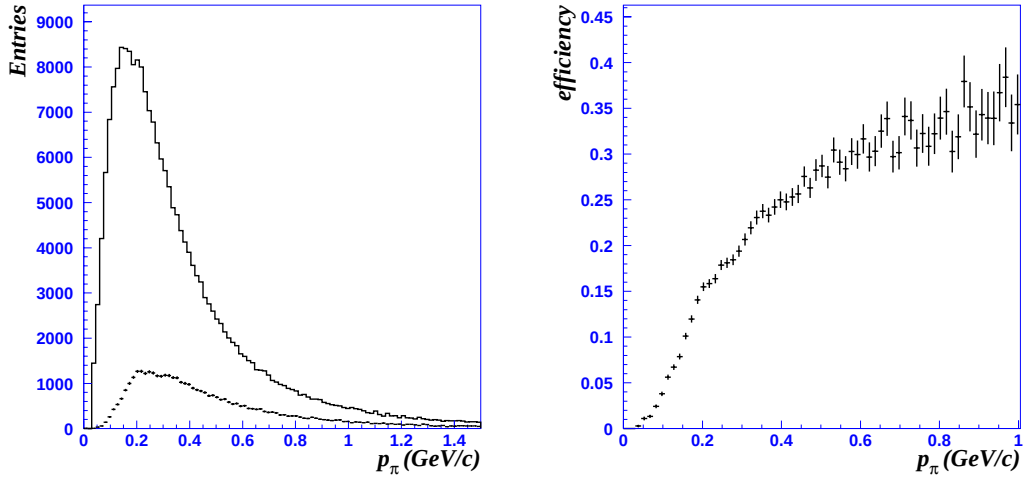

Figure 10: The π^- momentum distribution in generated (solid line) and reconstructed (crosses) Λ decays (left). The reconstruction efficiency of $\Lambda \to p\pi^-$ decays as a function of the pion momentum (right).

3.2 Standard method of polarization measurement

The method most frequently used to extract the Λ polarization (taking into account the detector acceptance) consists of histogramming the one dimensional *reconstructed* $\cos\theta_i$ distributions both for simulated events and data and by doing a least squares fit to their bin-by-bin ratio using a linear function (as illustrated in Fig. 11). We stress that

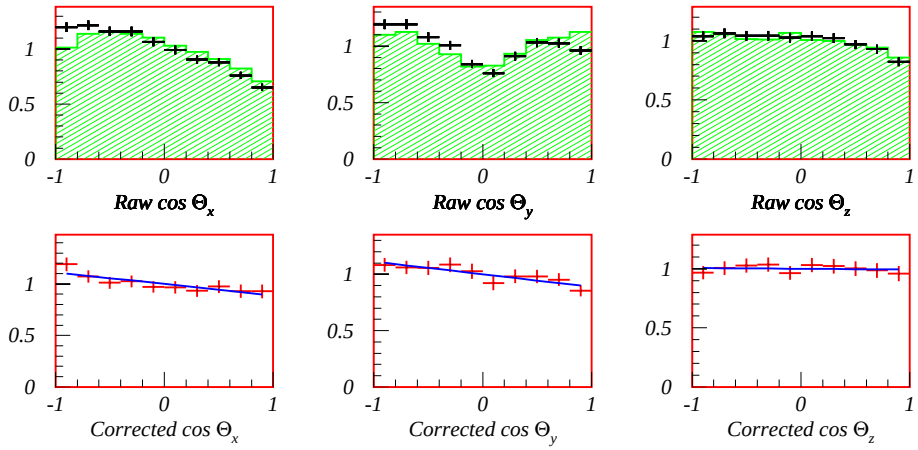

Figure 11: Top: normalized raw distributions of $\cos\theta_i$ for Λ's in reconstructed Monte Carlo events (histogram) and in the data (points with error bars). Bottom: angular distributions in the data after correction for detector acceptance; the polarization is given by the slope of the corresponding linear fit.

in this method each component of the polarization vector is extracted independently of the others. Moreover, smearing effects in the angular distributions due to reconstruction errors have to be taken into account, though the corresponding corrections are expected to be rather small (see Fig. 9).

3.3 Alternative method of polarization measurement

A method which allows the simultaneous extraction of all three components of the Λ polarization vector, taking into account differences between generated and reconstructed angular variables has been developed [42]. The essence of this method is the following. We introduce a "polarization" as three free parameters for *simulated* events, i.e. we associate an appropriate polarization weight to each Λ hyperon. We then try to fit the "polarized" MC angular distribution distorted by the detector acceptance to the angular distribution observed in the data. This is done varying all three components of the polarization vector $\mathbf{P}$ at the same time. The fit is performed by a MINUIT [43] based program with a minimization functional[1)] advocated in [44]:

$$\chi^2(\mathbf{P}) = 2 \cdot \sum_i \left[(N_i^{MC} - N_i^{data}) + N_i^{data} \ln(N_i^{data}/N_i^{MC}) \right] \tag{9}$$

where $N_i^{MC} = K f_i(\mathbf{P})$ is the renormalized MC content of the i-th bin, $K = N^{data}/N^{MC}$ is the global normalization factor, $f_i(\mathbf{P}) = W_i(\mathbf{P}) + N_i^{bg}$ is the sum of the polarization weight and the background contamination in the i-th bin predicted by MC simulation. The polarization weight for the i-th bin is calculated as follows:

$$W_i(\mathbf{P}) = \frac{N_i^{\Lambda}\,(1 + \alpha_\Lambda \mathbf{P} \cdot < \mathbf{k}^{sim} >_i)}{1 + \alpha_\Lambda \mathbf{P} \cdot < \mathbf{k}^{sim} >},$$

where $< \mathbf{k}^{sim} >_i$ and $< \mathbf{k}^{sim} >$ represent the *simulated* vector $\mathbf{k}^{sim}$ averaged over the i-th bin and over the total $\mathbf{k}$ space respectively.

We have performed the polarization analysis using two different types of binning:

- three dimensional (3D) binning on the surface of the sphere defined by $\mathbf{k}^2 = 1$;
- one dimensional (1D) binning for each projection independently.

We have verified that the correlations between different projections in the 3D case are small (the largest correlation, between P_x and P_z, is found to be less than 8%). The results obtained by the 3D and the 1D methods are similar.

In what follows we will present the results obtained using the 1D option of this method because of its better applicability to low statistics samples as is the case in the study of the polarization dependence on different kinematic variables.

3.4 Control sample

A useful control sample is provided by K_s^0 mesons which, being spinless, should not exhibit "polarization" along any direction. We have analyzed the K_s^0 sample by fitting the angular distributions of the decay π^+ in exactly the same manner as for the Λ's (while setting the decay asymmetry parameter to 1, see Fig. 12). Nevertheless, one should keep in mind that this check is necessary but not sufficient since the $K_s^0 \to \pi^+\pi^-$ decay is symmetric and its reconstruction is not biased by the loss of low energy negative pions (as is the case in $\Lambda \to p\pi^-$ decay, see Section 3.1) due to the larger average momenta of the decay pions.

[1)] other minimization functionals have been also used for cross-checks.

At each step of our analysis we have checked that the "polarization" of the K^0_s sample is consistent with zero (see results reported in subsection 4.6).

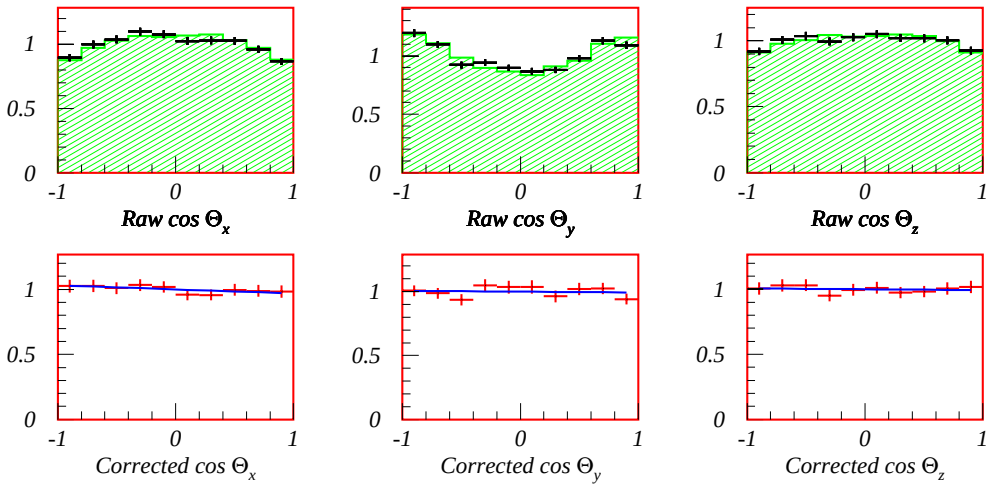

Figure 12: Top: normalized raw distributions of $\cos\theta_i$ for K^0_s's in reconstructed Monte Carlo events (histogram) and in the data (points with error bars). Bottom: angular distributions in the data after correction for detector acceptance.

4 RESULTS AND DISCUSSION

In this section we present the main results of our analysis. The Λ polarization measurement for the full data set is given in Table 5 together with the information on the quality of the fit. In what follows we omit this information but it has always been checked that the fitting procedure gives reasonable values for the normalized chi-squared.

Table 5: The Λ polarization measurements in ν_μ CC events (statistical errors only).

Selection	Entries	Λ Polarization		
		P_x	P_y	P_z
full sample	8087	-0.15 ± 0.03	-0.22 ± 0.03	-0.04 ± 0.03
χ^2/NDF		13.4/9	9.8/9	11.8/9

We observe a *negative* polarization along the W-boson direction (P_x) and in the direction orthogonal to the production plane (P_y). This is the first time that a neutrino experiment has observed a non-zero transverse polarization P_y.

4.1 Dependence on kinematic variables

The large statistics of our experimental data set allows the dependence of the polarization on several kinematic variables to be studied. We study the dependence of the polarization on x_F and on the square of the transverse momentum (p_T^2) with respect to the hadronic jet direction.

Figures 13 and 14 show a comparison of data and simulated events for these kinematic variables after the reconstruction and identification procedures. There is a general agreement between MC and data for these distributions. The initial x_F distributions of both Λ's and K^0_s's, which are mainly produced in the target and in the central fragmentation regions, respectively, are distorted by the detector acceptance. The smearing in x_F

distribution for Λ's could cause a migration of events from the region $x_F < 0$ to the region $x_F > 0$ and vice versa. In the MC simulation we find that the number of events coming from the other region is 12% (3%) of the total number of events in the current (target) fragmentation region.

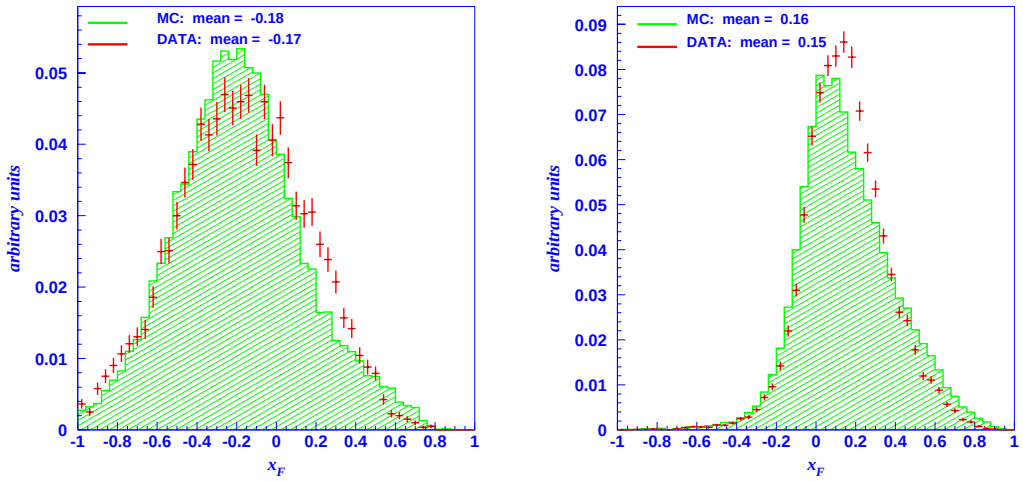

Figure 13: Normalized x_F distribution for reconstructed Λ (left) and K^0_s (right): comparison of data (points with error bars) and MC with full detector simulation (histogram).

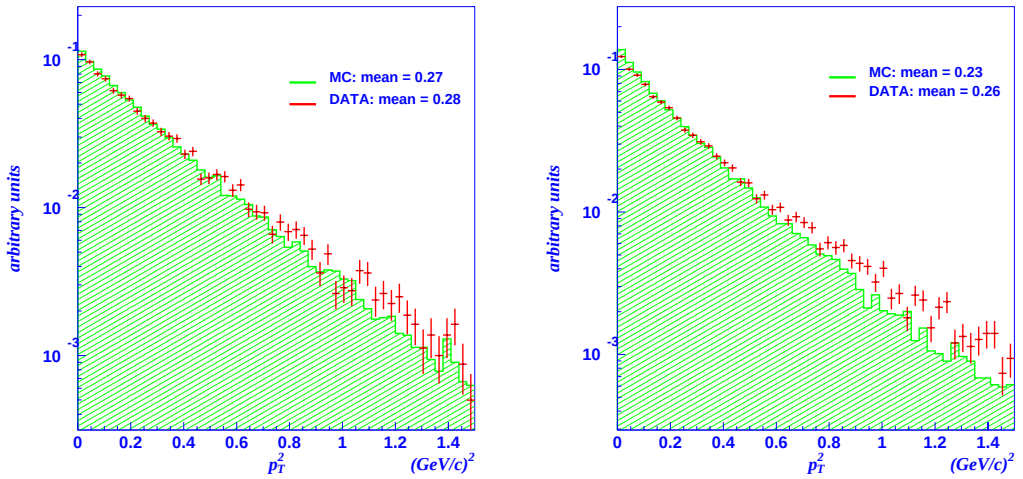

Figure 14: Normalized p_T^2 distribution for reconstructed Λ (left) and K^0_s (right): comparison of data (points with error bars) and MC with full detector simulation (histogram). An approximately exponential fall is evident in these distributions below 0.5 $(\mathrm{GeV}/c)^2$.

4.2 Dependence of the polarization on x_F

As discussed in Section 1.2 different physical mechanisms are responsible for the Λ polarization in the target and in the current fragmentation regions. Imposing cuts on x_F, we obtain the results presented in Table 6. The absolute value of the longitudinal polarization P_x is larger in the target fragmentation region ($x_F < 0$) than in the current fragmentation region ($x_F > 0$).

Table 6: Dependence of the Λ polarization on x_F in ν_μ CC events (statistical errors only).

Selection	Entries	$< x_F >$	Λ Polarization		
			P_x	P_y	P_z
full sample	8087	-0.18	-0.15 ± 0.03	-0.22 ± 0.03	-0.04 ± 0.03
$x_F < 0$	5608	-0.36	-0.21 ± 0.04	-0.26 ± 0.04	-0.08 ± 0.04
$x_F > 0$	2479	0.21	-0.09 ± 0.06	-0.10 ± 0.06	0.02 ± 0.06

Figure 15 shows the behaviour of both the longitudinal and transverse polarization as a function of x_F. We note that the absolute value of the transverse polarization P_y, like P_x, is larger in the target fragmentation region than in the current fragmentation region.

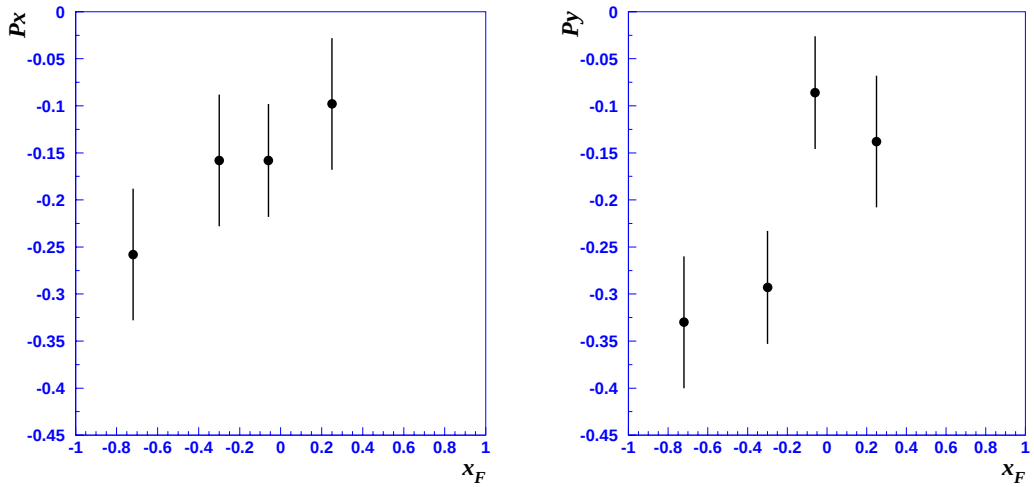

Figure 15: Dependence of longitudinal (left) and transverse (right) polarization of Λ-hyperons on x_F.

We have also studied the z dependence of the Λ polarization (where $z = E(\Lambda)/E$ (all hadrons) is the fraction of the total hadronic energy carried away by the Λ in the laboratory system) as well as its y_B dependence in the current fragmentation region (see Table 7). This study is motivated by different z-dependences of the Λ polarization being predicted in various theoretical models of the spin transfer mechanism. As already stated in Section 1.2.2, the measurement of the Λ polarization in the region $y_B \to 1$ could provide a direct measurement of the spin transfer coefficient $C_u^\Lambda = \frac{\Delta D_u^\Lambda(z)}{D_u^\Lambda(z)}$ (for Λ's which are produced directly and from the decay of heavier baryons). However Table 7 shows that the y_B dependence of the polarization is weak, which agrees with the smallness of the $\bar{u}$ contribution with respect to the one of the d quark (see Eq. 6). Thus we can interpret our measurement of the longitudinal Λ polarization as an estimate of the spin transfer coefficient $C_u^\Lambda = -P_x = 0.09 \pm 0.06(\text{stat})$. The effect of the x_F smearing (discussed in Section 4.1) on the polarization measurement is smaller than the statistical error.

4.3 Dependence of the polarization on x_B, W^2, Q^2

We have also studied the dependence of the polarization on other kinematic variables, such as x_B, W^2, Q^2 (see Table 8). The idea here is to try to find a kinematic region in which the polarization is enhanced.

Table 7: The Λ polarization measurements in ν_μ CC events in the current fragmentation region (statistical errors only).

Selection	Entries	$< z >$	Λ Polarization		
			P_x	P_y	P_z
$z < 0.42$	1221	0.30	-0.16 ± 0.08	-0.04 ± 0.09	0.06 ± 0.09
$z > 0.42$	1258	0.57	-0.01 ± 0.08	-0.17 ± 0.09	-0.03 ± 0.09
$y_B < 0.47$	1228	0.49	-0.07 ± 0.08	-0.13 ± 0.09	-0.13 ± 0.09
$y_B > 0.47$	1251	0.39	-0.10 ± 0.08	-0.07 ± 0.09	0.15 ± 0.09

Table 8: Dependence of the polarization on x_B, W^2 and Q^2 in ν_μ CC events (statistical errors only).

Selection	Entries	Λ Polarization		
		P_x	P_y	P_z
$x_B < 0.2$	3508	-0.15 ± 0.05	-0.17 ± 0.05	-0.11 ± 0.05
$x_B > 0.2$	4579	-0.15 ± 0.04	-0.26 ± 0.04	0.00 ± 0.05
$W^2(\mathrm{GeV}^2) < 15$	2755	-0.34 ± 0.06	-0.25 ± 0.06	-0.08 ± 0.06
$W^2(\mathrm{GeV}^2) > 15$	5332	-0.06 ± 0.04	-0.21 ± 0.04	-0.03 ± 0.04
$Q^2(\mathrm{GeV}^2) < 5$	3429	-0.21 ± 0.05	-0.20 ± 0.05	-0.08 ± 0.05
$Q^2(\mathrm{GeV}^2) > 5$	4658	-0.11 ± 0.04	-0.24 ± 0.04	-0.02 ± 0.04

One could expect a dependence of the polarization on x_B due to the contribution from sea (anti)quarks to the Λ production at small x_B. Contrary to some previous measurements performed with bubble chambers [32], we have not found any statistically significant dependence of the longitudinal polarization on x_B.

Some enhancement of the longitudinal polarization is observed at low W^2 ($W^2 <$ 15 GeV^2) and at low Q^2 ($Q^2 < 5$ GeV^2), while the transverse polarization does not seem to depend significantly on these variables. This effect could have a simple interpretation in the framework of the model of polarized $s\bar{s}$ pairs in the nucleon: at low $W^2(Q^2)$ there is a higher chance that the s quark which was originally in the target nucleon will become a valence quark of the Λ, while at high $W^2(Q^2)$ the s quark in the Λ is likely to be created in the fragmentation process.

4.4 Dependence of the polarization on p_T

We wish to emphasize another important feature of the results presented here: the presence of the negative transverse Λ polarization. As was pointed out in the review of experimental data (Section 1.3), previous neutrino experiments had not reported any statistically significant dependence of the polarization on the transverse momentum of the Λ with respect to the hadronic jet direction (p_T). On the contrary, a strong dependence of the transverse polarization on the transverse momentum of Λ with respect to the incoming beam direction has been firmly established in hadron-hadron experiments (see Fig. 16).

The *transverse* polarization of Λ hyperons produced in inclusive interactions of unpolarized protons with unpolarized targets over a wide range of energies and production angles has been studied over the last decades. The absolute value of the polarization has been found to grow approximately linearly with p_T (see Fig. 16 taken from [45] as an example) and x_F. Some theoretical models (see [46, 47] and references therein)

attempt to describe the transverse polarization but the polarization mechanism is still not understood.

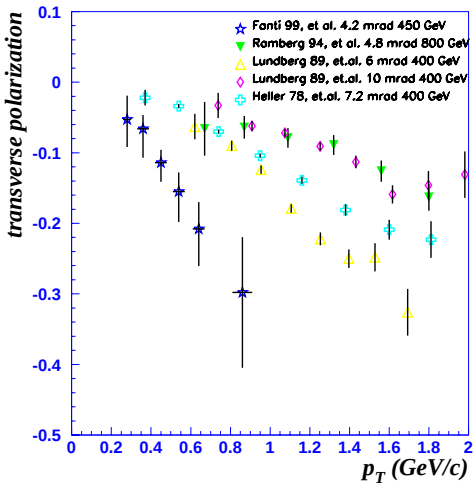

Figure 16: The measured dependence of the transverse Λ polarization on p_T in hadron-hadron experiments.

We have performed a similar study of the transverse polarization, obtaining the results presented in Table 9 and shown in Fig. 17. The absolute value of the measured transverse polarization increases with increasing p_T of the Λ with respect to the hadronic jet. This is the first observation of such an effect with small statistical errors in neutrino experiments and it is in qualitative agreement with hadron-hadron measurements.

Table 9: Dependence of the Λ polarization on p_T in ν_μ CC events (statistical errors only).

Selection (p_T^2 in $(\mathrm{GeV}/c)^2$)	Entries	$< p_T >$ GeV/c	Λ Polarization		
			P_x	P_y	P_z
$p_T^2 < 0.06$	1629	0.16	-0.25 ± 0.08	-0.02 ± 0.08	-0.06 ± 0.08
$0.06 < p_T^2 < 0.15$	1712	0.32	-0.35 ± 0.07	-0.19 ± 0.07	-0.02 ± 0.07
$0.15 < p_T^2 < 0.28$	1669	0.46	0.01 ± 0.07	-0.30 ± 0.07	-0.00 ± 0.07
$0.28 < p_T^2 < 0.55$	1746	0.62	-0.01 ± 0.07	-0.31 ± 0.06	-0.06 ± 0.07
$0.55 < p_T^2$	1332	0.95	-0.25 ± 0.08	-0.25 ± 0.08	-0.11 ± 0.08

The transverse polarization observed in ν DIS formally has an opposite direction compared to hadron-hadron experiments given the difference in the definition of the y-axis in these two cases. Indeed, by convention, the axis orthogonal to the production plane is defined in hadron-hadron experiments as $\mathbf{n}_y = \vec{e}_{beam} \times \vec{e}_\Lambda$, while the "J" reference system used in neutrino experiments assumes the following construction of the y-axis: $\mathbf{n}_y = \vec{e}_W \times \vec{e}_T$ which is equivalent to $\mathbf{n}_y = \vec{e}_\Lambda \times \vec{e}_W$ (or to $\mathbf{n}_y = \vec{e}_\Lambda \times \vec{e}_\nu$ in the "ν" reference system). As one can see, the direction of the y-axis is opposite in these two cases. However, the results presented in Fig. 16 correspond to the region $x_F > 0$, while the NOMAD data (Fig. 17) correspond mainly to the region $x_F < 0$. Thus taking into account the opposite directions of motion of Λ's in the W boson-nucleon and in the hadron-hadron centre-of-mass systems, the *physical* vectors of the transverse polarization point in the same direction for both the NOMAD and hadron-hadron experiments.

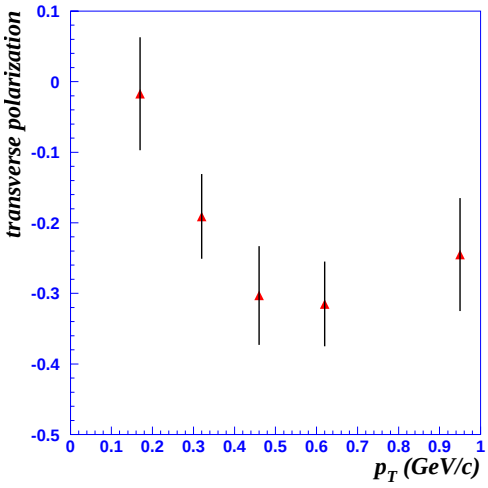

Figure 17: The dependence of the transverse Λ polarization on p_T observed in the NOMAD experiment.

Another firmly established result of hadron-hadron experiments is the *increase* of the slope of the transverse polarization dependence on p_T at larger absolute values of x_F [47]. Our data do not allow for a detailed study of this effect. However, we can state that the mean value of the transverse polarization shows a similar behaviour (see P_y dependence on x_F in Fig. 15).

The behaviour of the absolute value of the longitudinal polarization is also interesting (see Table 9). Contrary to the transverse polarization, the longitudinal one is large at low p_T values, it vanishes in the region where the transverse polarization reaches a plateau and increases again at larger p_T values.

The behaviour of the Λ polarization vector in the $\{xy\}$ plane of the "J" reference system in different p_T intervals can be seen in Fig. 18.

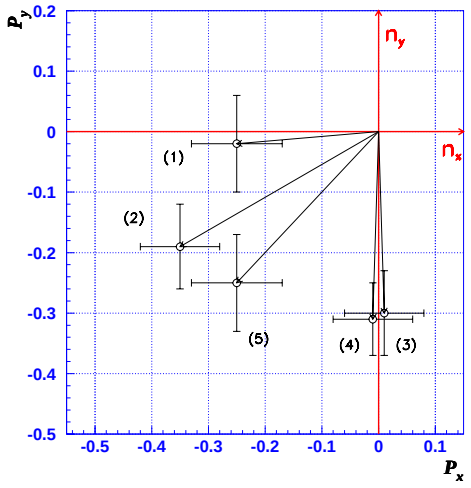

Figure 18: The behaviour of the Λ polarization vector in the $\{xy\}$ plane in different p_T intervals: notations (1)-(5) correspond to the order of selection in Table 9.

4.5 Dependence of the polarization on the type of target nucleon

A possible way to investigate the origin of the Λ polarization is to study its dependence on the type of target nucleon. In NOMAD it is possible to separate neutrino interactions on neutrons and protons by using the sum of charges (Q_{tot}) of all the outgoing tracks at the primary neutrino interaction vertex.

We select νp events by requiring $Q_{tot} \geq 1$. The corresponding sample of proton-like events contains about 76% of true νp interactions. The νn events are selected by the requirement $Q_{tot} \leq 0$. The purity of the corresponding neutron-like sample is about 85%.

The results of the Λ polarization measurements in the proton-like and neutron-like samples are summarized in Table 10. One can conclude that there is a strong dependence of the Λ polarization on the type of target nucleon: while negative longitudinal polarization is observed in both cases, the absolute value of the longitudinal polarization is smaller for neutron-like than for proton-like events. Such a dependence could be attributed to the difference between the Λ production mechanisms in νp and νn DIS.

Table 10: The dependence of the Λ polarization on the type of target nucleon.

Target	Entries	Λ Polarization		
		P_x	P_y	P_z
"proton"	3472	-0.26 ± 0.05	-0.09 ± 0.05	-0.07 ± 0.05
$x_F < 0$	2407	-0.29 ± 0.06	-0.10 ± 0.06	-0.09 ± 0.06
$x_F > 0$	1065	-0.23 ± 0.09	-0.06 ± 0.09	-0.02 ± 0.10
"neutron"	4615	-0.09 ± 0.04	-0.30 ± 0.04	-0.03 ± 0.05
$x_F < 0$	3201	-0.16 ± 0.05	-0.37 ± 0.05	-0.07 ± 0.05
$x_F > 0$	1414	0.01 ± 0.08	-0.11 ± 0.08	0.04 ± 0.09

Indeed, according to the LUND model predictions[2)] for the conditions of the NOMAD experiment, the fraction of prompt Λ's produced in νn DIS is about 55%, while the fraction of prompt Λ's produced in νp DIS is about 29% with major additional contributions coming from $\Sigma^{\star+}$ resonance (about 36%) and Σ^0 decay (about 16%). More details can be found in Table 11.

Table 11: The origin of Λ's as predicted by the LUND model.

Target	Fraction of Λ's, %				
	prompt	Σ^0	$\Sigma^{\star+}$	$\Sigma^{\star0}$	$\Sigma^{\star-}$
p	28.6	15.6	35.8	11.0	0.2
n	54.6	13.0	8.0	10.8	7.3

Therefore, the longitudinal polarization in νn DIS is more sensitive to the intrinsic nucleon strangeness discussed in Section 1.2.1, while in νp DIS a considerable fraction of the Λ polarization is inherited from the decay of heavier baryons. The most important contribution to the Λ polarization in νp DIS is due to the $\Sigma^{\star+}$ resonance because of the following reasons:

– the uu pair from the target proton carries spin equal to 1 aligned in the opposite direction to the spin of the struck d quark;

[2)] with default JETSET parameters used in our MC simulation.

– the $\Sigma^{\star+}$ polarization is defined mainly by the polarization of the uu pair inside the $\Sigma^{\star+}$ hyperon;
– the polarization of Λ's which are decay products of $\Sigma^{\star+}$ resonances is the same as that of the $\Sigma^{\star+}$ [20];
– finally, the fraction of Λ's coming from the $\Sigma^{\star+}$ decay is quite sizeable, even taking into account a possible difference of the $\Sigma^{\star+}$ production between data and MC predictions.

One should stress that detailed theoretical calculations in the framework of different models of baryon spin content, together with experimental measurements of yields of relevant resonances and heavier baryons (see discussion in [48] for example) are required for the interpretation of our Λ polarization measurements. However, we can state that the measured longitudinal Λ polarization in the neutron-like sample is more directly related to the polarized strange content of the nucleon than the one measured in the proton-like sample.

Another very interesting observation, which follows from Table 10, is the dependence of the transverse Λ polarization on the type of target nucleon. It is opposite to that of the longitudinal polarization: the absolute value of the transverse polarization is larger in the neutron-like than in the proton-like sample. This feature can also be attributed to the different Λ production mechanisms discussed above. Although the physical origin of the transverse Λ polarization is not well understood, one can assume it to be related to the fragmentation process of the s quark into the Λ. If this is indeed the case, this effect is more significant for prompt Λ's, than for those coming from the decay of heavier baryons, because only a small fraction of the original s quark polarization is carried on by the Λ.

4.6 Results for the K^0_s sample

The K^0_s mesons, being spinless and having the same decay topology as the Λ hyperons, provide a good way to verify that the polarization analysis is free of obvious biases. As a cross-check we give in Table 12 the results obtained for the selected K^0_s sample.

Table 12: The K^0_s "polarization" for different kinematic selections (statistical errors only).

Selection	Entries	K^0_s "Polarization"		
		P_x	P_y	P_z
full sample	15074	-0.04 ± 0.02	-0.02 ± 0.02	-0.02 ± 0.02
$x_F < 0$	3252	-0.04 ± 0.03	-0.01 ± 0.03	0.03 ± 0.04
$x_F > 0$	11822	-0.04 ± 0.02	-0.02 ± 0.02	-0.02 ± 0.02
$x_B < 0.2$	7575	-0.05 ± 0.02	-0.02 ± 0.02	0.00 ± 0.02
$x_B > 0.2$	7499	-0.04 ± 0.02	-0.01 ± 0.02	-0.04 ± 0.02
$W^2(\mathrm{GeV}^2) < 15$	2787	-0.05 ± 0.04	0.01 ± 0.04	0.02 ± 0.04
$W^2(\mathrm{GeV}^2) > 15$	12287	-0.04 ± 0.02	-0.02 ± 0.02	-0.03 ± 0.02
$Q^2(\mathrm{GeV}^2) < 5$	5350	-0.05 ± 0.03	-0.05 ± 0.03	0.00 ± 0.03
$Q^2(\mathrm{GeV}^2) > 5$	9724	-0.04 ± 0.02	-0.00 ± 0.02	-0.03 ± 0.02

5 SYSTEMATIC ERRORS AND CHECKS

The following potential sources of systematic errors have been studied in the present analysis:
– uncertainty in the incoming neutrino energy determination, which could result in an uncertainty in the reconstructed W-boson direction and, thus, lead to a poor

definition of the main reference system ("J" system) in which the Λ polarization is measured;
- poor knowledge of relative background rates caused by possible differences between simulated events and data;
- potential dependence of final results on the selection criteria;
- spin precession for a particle travelling through a magnetic field;
- smearing of the x_F distribution;
- possible effects related to background contamination from ν neutral current (NC) interactions.

The uncertainty in the evaluation of the incoming neutrino energy affects the definition of the axes and thus essentially the polarization direction, but also slightly the magnitude of the polarization itself. To obtain an estimate of the systematic uncertainty which should be attributed to the knowledge of the incoming neutrino energy we have repeated the analysis using three different methods of neutrino energy calculation: total visible energy, Myatt[3)] approach [49] and double angle[4)] method [50]. The results are very similar and the corresponding systematic uncertainties are given in the first column of Table 13. Here and in what follows, we estimate the systematic uncertainty as the largest deviation obtained with respect to the reference result.

The background fraction in the sample of selected Λ candidates is not constant as a function of the angular variables, thus a possible difference in the background contribution between data and MC predictions can lead to a fake "polarization". It is possible to estimate this difference by comparing yields of both identified V^0 and fake V^0-like vertices (random track associations, neutron interactions, etc) in specific kinematic regions. Using this approach it has been found that V^0 yields in the data exceed the MC predictions by the following factors: 1.1 for K^0_s, 2.0 for γ, and 2.1 for fake V^0's [37]. The systematic uncertainty due to background contamination (see the second column of Table 13) has been evaluated using the method described in section 3.3 with Monte Carlo predicted background V^0 samples, increased by the factors given above.

Table 13: Summary of systematic errors on the three components of the Λ polarization vector.

P_i	ν energy reconstruction	V^0 induced background	variation of cuts	spin precession	total
P_x	$3.4 \cdot 10^{-3}$	$3.5 \cdot 10^{-3}$	$1.7 \cdot 10^{-2}$	$1.4 \cdot 10^{-3}$	$1.8 \cdot 10^{-2}$
P_y	$8.5 \cdot 10^{-3}$	$4.9 \cdot 10^{-3}$	$3.8 \cdot 10^{-3}$	$7.2 \cdot 10^{-5}$	$1.1 \cdot 10^{-2}$
P_z	$1.2 \cdot 10^{-2}$	$7.8 \cdot 10^{-3}$	$1.2 \cdot 10^{-2}$	$8.6 \cdot 10^{-4}$	$1.9 \cdot 10^{-2}$

To check the stability of the results we have varied the selection criteria in the following range: p_T^{int} from 0.01 to 0.03 GeV/c, p_T^{dirv} from 0.075 to 0.125 GeV/c and W^2 up to 2.5 GeV^2. We have also checked the stability of the polarization results with respect to changes of the fiducial volume (for example, the analysis has been performed with a

[3)] The incoming neutrino energy is computed as $E_\nu = p_L^\mu + p_L^{had} \cdot \frac{p_T^\mu}{p_T^{had}}$, where p_L^μ (p_L^{had}) and p_T^μ (p_T^{had}) are the longitudinal and transverse momenta of the muon (all the detected hadrons) with respect to the incoming neutrino direction.

[4)] The incoming neutrino energy is computed according to the following formula $E_\nu = E_\mu \frac{\sin\gamma+\sin\theta+\sin(\gamma+\theta)}{2\sin\gamma}$, where E_μ is the energy of the muon and θ (γ) is the muon (hadronic jet) polar angle with respect to the neutrino direction.

cut on the primary vertex position $|X, Y| < 110$ cm and 50 cm $< Z <$ 395 cm and no difference has been found within statistics). The importance of these effects on the final result can be found in the third column of Table 13.

The effect of the Λ spin precession in the NOMAD magnetic field has been calculated to be very small (the Λ spin is rotated by $\sim 1.7^o$ on average). Our estimate of this source of systematic error can be found in the fourth column of Table 13.

Smearing effects in the measurement of x_F lead to a migration of Λ's from the target to the current fragmentation region (and vice versa). This effect is more important for the polarization measurement in the current fragmentation region because of the asymmetry in the x_F distribution for Λ's (see Fig. 13) and due to the fact that the absolute value of the polarization is larger in the $x_F < 0$ region. We estimate the error related to this effect as

$$\frac{\text{Number of } \Lambda\text{'s from } x_F < 0 \text{ migrated to } x_F > 0}{\text{Number of } \Lambda\text{'s in } x_F > 0} \times \text{Polarization of } \Lambda\text{'s in } x_F < 0.$$

The systematic errors due to the x_F smearing effect are: 0.025 for the current fragmentation region and 0.005 for the target fragmentation region.

Systematic errors introduced by a possible contamination from ν NC events (with a hadron decaying into a muon) in the sample of selected Λ's have also been studied. We have analyzed a large sample of ν_μ NC MC events with the criteria used in this analysis. Normalizing to the expected number of ν NC events in our data sample we obtain $\sim 20 \div 30$ events which are randomly distributed in the angular regions of interest. Thus, the contamination from ν NC events is less than 0.5% in the sample of selected Λ's and represents a negligible background for the analysis of the Λ polarization presented here.

Using the MC, it has been checked that the presence of Fermi motion does not affect the Λ polarization measurements.

By comparing the results obtained for different periods of data taking, one can get an estimate of the systematic uncertainty due to the detector calibration (mainly the alignment quality of the drift chambers and the stability of the electromagnetic calorimeter response). The results of the polarization analysis for each year of data taking agree within statistics.

It is important to note that the polarization analysis has been repeated with the event sample containing only uniquely identified Λ's. The corresponding measurements are in good agreement with the reference results.

A summary of all the systematic errors is given in Table 13 for the full sample. A conservative[5)] estimate of the systematic error is obtained by adding all the contributions in quadrature. The systematic error has been calculated in the same way for all the kinematic selections used in this study. The value of the systematic error can reach 0.05 in some kinematic regions.

An additional check has been made considering alternative coordinate systems and comparing the absolute value of the total polarization vector measured in different systems. We have verified that there is a strong correlation between the $\vec{e}_W$, $\vec{e}_T$ and $\vec{e}_\nu$ vectors.

The following coordinate systems have been defined (in the Λ rest frame):

– "T" system:

$$\mathbf{n}_x = -\vec{e}_T, \ \mathbf{n}_y = \vec{e}_W \times \vec{e}_T, \ \mathbf{n}_z = \mathbf{n}_x \times \mathbf{n}_y$$

[5)] Neglecting possible correlations between variation of cuts and V^0 induced background estimates.

– "ν" system (note that this system is free from uncertainties in the incoming neutrino energy determination):

$$\mathbf{n}_x = \vec{e}_\nu,\ \mathbf{n}_y = \vec{e}_\nu \times \vec{e}_T,\ \mathbf{n}_z = \mathbf{n}_x \times \mathbf{n}_y$$

It was found that because of a strong correlation between the W-boson and the incoming neutrino directions, the "J"("T") and "ν" systems have on average a common y-axis, that is, one system can be obtained from the other one by a simple rotation around this common y-axis. The determination of the absolute value and the direction of the total polarization vector gives consistent results in all three systems (see Table 14). This can be considered as another independent check of the results of this analysis.

Table 14: Dependence of the Λ polarization on the choice of the reference system (statistical errors only).

Reference frame	Λ Polarization			
	P_x	P_y	P_z	$\lvert P_{\rm tot}\rvert$
"J" system	-0.15 ± 0.03	-0.22 ± 0.03	-0.04 ± 0.03	0.27 ± 0.03
"T" system	-0.17 ± 0.03	-0.22 ± 0.03	0.08 ± 0.03	0.29 ± 0.03
"ν" system	-0.10 ± 0.03	-0.19 ± 0.03	-0.14 ± 0.03	0.26 ± 0.03

6 SUMMARY AND CONCLUSION

The full sample of ν_μ CC data of the NOMAD experiment has been analyzed. A kinematic fit has been used for the identification of neutral strange particles. The results obtained are stable with respect to changes in the V^0 identification procedure. The method used to extract the three components of the Λ polarization vector automatically accounts for the smearing of the angular variables.

Results of the analysis are given in the "J" reference system, which is found to be the only system in which the P_z component of the polarization is always consistent with zero. We observe *negative* polarization along the W-boson direction (P_x) and in the direction orthogonal to the production plane (P_y). This is the *first* time that a neutrino experiment has observed a non-zero transverse polarization P_y.

The longitudinal polarization is enhanced in the target fragmentation region ($x_F < 0$): $P_x = -0.21 \pm 0.04(\text{stat}) \pm 0.02(\text{sys})$, while in the current fragmentation region ($x_F > 0$) the longitudinal polarization is found to be $P_x = -0.09 \pm 0.06(\text{stat}) \pm 0.03(\text{sys})$. A similar dependence on x_F is observed for the transverse polarization.

The result obtained for the longitudinal polarization in the current fragmentation region provides a measurement of the spin transfer coefficient $C_u^\Lambda = -P_x = 0.09 \pm 0.06(\text{stat}) \pm 0.03(\text{sys})$ at $< z >= 0.44$.

There is an enhancement of the longitudinal polarization in both low W^2 ($W^2 < 15$ GeV^2) and low Q^2 ($Q^2 < 5$ GeV^2) regions, while P_y does not seem to depend on these selections. For example, $P_x = -0.34 \pm 0.06(\text{stat}) \pm 0.02(\text{sys})$ at $W^2 < 15$ GeV^2. No statistically significant dependence of the longitudinal polarization upon x_B has been found.

Both P_x and P_y depend strongly on the p_T of the Λ with respect to the hadronic jet direction. The maximum values obtained are:

$P_x = -0.35 \pm 0.07(\text{stat}) \pm 0.05(\text{sys})$ at $0.06 < p_T^2 < 0.15$ (GeV^2)

$P_y = -0.31 \pm 0.06(\text{stat}) \pm 0.04(\text{sys})$ at $0.28 < p_T^2 < 0.55$ (GeV^2)

The dependence of the absolute value of the transverse polarization on p_T is in qualitative agreement with the results of unpolarized hadron-hadron experiments (see Figs. 16 and 17).

The dependence of the polarization vector on the type of target nucleon (proton or neutron) has also been studied. The longitudinal polarization in the proton-like sample is negative and is enhanced in comparison with the total event sample. This can be interpreted as due to Λ's coming from the decay of $\Sigma^{\star+}$ and other heavier baryons. The measured longitudinal polarization in the neutron-like sample is also negative and probably more directly related to the polarized strange content of the nucleon. The transverse polarization is more evident in the neutron-like sample, where most Λ's are produced promptly, and therefore the properties of the strange quark originating from the nucleon are likely to be conserved.

The theoretical interpretation of the results reported in this article should take into account the effects of secondary Λ's originating from the decays $\Sigma^\star \to \Lambda\pi$, $\Sigma^0 \to \Lambda\gamma$ and $\Xi \to \Lambda\pi$ where the polarization of the secondary Λ's is inherited from the polarization of the parent particles and is different from the polarization of the directly produced Λ's.

Acknowledgements

We gratefully acknowledge the CERN SPS accelerator and beam-line staff for the magnificent performance of the neutrino beam. The experiment was supported by the following funding agencies: Australian Research Council (ARC) and Department of Industry, Science, and Resources (DISR), Australia; Institut National de Physique Nucléaire et Physique des Particules (IN2P3), Commissariat à l'Energie Atomique (CEA), France; Bundesministerium für Bildung und Forschung (BMBF, contract 05 6DO52), Germany; Istituto Nazionale di Fisica Nucleare (INFN), Italy; Joint Institute for Nuclear Research and Institute for Nuclear Research of the Russian Academy of Sciences, Russia; Fonds National Suisse de la Recherche Scientifique, Switzerland; Department of Energy, National Science Foundation (grant PHY-9526278), the Sloan and the Cottrell Foundations, USA.

We are grateful to A. Kotzinian, I. Bigi, and A. Efremov for stimulating discussions on different theoretical models of nucleon spin content and to Yu. Merekov for the help in the kinematic fit implementation.

References

[1] J.Altegoer *et al.*, [NOMAD Collaboration], Nucl. Instr. and Meth. **A404** (1998) 96.

[2] J.Altegoer *et al.*, [NOMAD Collaboration], Phys. Lett. **B431** (1998) 219.
P.Astier *et al.*, [NOMAD Collaboration], Phys. Lett. **B453** (1999) 169.

[3] G.Ingelman, LEPTO version 6.1, "The Lund Monte Carlo for Deep Inelastic Lepton-Nucleon Scattering", TSL-ISV-92-0065 (1992);
G.Ingelman, A.Edin, J.Rathsman, LEPTO version 6.5, Comp. Phys. Comm. **101** (1997) 108, hep-ph/9605286.

[4] T.Sjöstrand, "PYTHIA 5.7 and JETSET 7.4: physics and manual", LU-TP-95-20 (1995); hep-ph/9508391;
T.Sjöstrand, Comp. Phys. Comm **39** (1986) 347, **43** (1987) 367.

[5] GEANT : Detector Description and Simulation Tool, *CERN Programming Library Long Writeup* **W5013**, GEANT version 3.21 (1994).

[6] M.Anfreville *et al.*, "The drift chambers of the NOMAD experiment", to be submitted to Nucl. Instr. and Meth.

[7] D.Autiero *et al.*, Nucl. Instr. and Meth. **A373** (1996) 358;
D.Autiero *et al.*, Nucl. Instr. and Meth. **A387** (1997) 352;
D.Autiero *et al.*, Nucl. Instr. and Meth. **A411** (1998) 285.
[8] Review of Particle Properties, Eur. Phys. J. **C3** (1998).
[9] J.Ashman *et al.*, [EMC Collaboration], Phys. Lett. **B206** (1988) 364;
Nucl. Phys. **B328** (1989) 1.
[10] D.Adams *et al.* [SMC Collaboration], Phys. Rev. **D56** (1997) 5330;
B.Adeva *et al.*, [SMC Collaboration], Phys. Lett. **B420** (1998) 180.
[11] A.Efremov, O.Teryaev, JINR preprint, JINR-E2-88-287;
G.Altarelli, G.Ross, Phys. Lett. **B212** (1988) 391;
R.Carlitz, J.Collins, A.Mueller, Phys. Let. **B214** (1988) 229.
[12] R.L.Jaffe and A.Manohar, Nucl. Phys. **B337** (1990) 509.
[13] K.Abe *et al.*, [E143 Collaboration], Phys. Rev. **D58** (1998) 112003.
[14] K.Ackerstaff *et al.*, [HERMES Collaboration], Phys. Lett. **B464** (1999) 123.
[15] J.Ellis, D.Kharzeev, A.Kotzinian, Z. Phys. **C69** (1996) 467.
[16] J.Ellis, M.Karliner, D.E.Kharzeev and M.G.Sapozhnikov, hep-ph/9909235.
[17] M.A.Shifman, A.I.Vainshtein, V.I.Zakharov, Nucl. Phys. **B147** (1979) 385, 448, 519;
B.L.Ioffe, Nucl. Phys. **B188** 317 [Erratum: **B191** (1981) 591];
L.J.Reinders, H.Rubinshtein, S.Yazaki, Phys. Rep. **127** (1985) 1.
[18] I.Bigi, Nuovo Cim. **41A** (1977) 581.
[19] M.Burkardt and R.L.Jaffe, Phys. Rev. Lett. **70** (1993) 2537.
[20] G.Gustafson and J.Häkkinen, Phys. Lett. **B303** (1993) 350.
[21] D.Buskulic *et al.*, [ALEPH Collaboration], Phys. Lett. **B374** (1996) 319.
[22] K.Ackerstaff *et al.*, [OPAL Collaboration], Eur. Phys. J. **C2** (1998) 49.
[23] A.Kotzinian, A.Bravar, D.von Harach, Eur. Phys. J. **C2** (1998) 329.
[24] C.Boros and Liang Zou-tang, Phys. Rev. **D57** (1998) 4491.
[25] D.de Florian, M.Stratmann and W.Vogelsang, Phys. Rev. Lett. **81** (1998) 530.
[26] R.L.Jaffe, Phys. Rev. **D 54** (1996) R6581.
[27] A.Airapetian *et al.*, [HERMES Collaboration], DESY-99-151 (1999);
hep-ex/9911017.
[28] M.R.Adams *et al.*, [E665 Collaboration], hep/ex9911004.
[29] G.Baum *et al.*, [COMPASS Collaboration], CERN-SPSLC-96-14 (1996).
[30] B.Ma and J.Soffer, Phys. Rev. Lett. **82** (1999) 2250.
[31] B.Ma, I.Schmidt, J.Soffer and J.Yang, hep-ph/0001259.
[32] G.T.Jones *et al.*, Z. Phys. **C28** (1985) 23.
[33] S.Willocq *et al.*, Z. Phys. **C53** (1992) 207.
[34] D.DeProspo *et al.*, Phys. Rev. **D50** (1994) 6691.
[35] V.Ammosov *et al.*, Nucl. Phys. **B162** (1980) 205.
[36] D.Allasia *et al.*, Nucl. Phys. **B224** (1983) 1.
[37] C.Lachaud, PhD Thesis, Université Denis Diderot (Paris 7), May 2000, *in french*
[38] R.Boeck, CERN preprint 60-30.
[39] J.P.Berge *et al.*, Review of Sci. Instr. **32** (1961) 538.
[40] O.I.Dahl *et al.*, UCRL, Group A Prog. Note **P-126** (1968).
[41] B.Ronne, CERN preprint 64-13.
[42] D.V.Naumov, PhD Thesis, JINR, Dubna, Russia (2000) *in russian.*
[43] MINUIT package, *CERN Program Library Long Writeup* **D506** (1992).
[44] S.Baker and R.Cousins, Nucl. Instr. and Meth. **221** (1984) 437.
[45] V.Fanti *et al.*, [NA48 Collaboration], Eur. Phys. J. **C6** (1999) 265.

[46] A.D.Panagiotou, Int. J. Mod. Phys. **A5** (1990) 1197.
[47] J.Félix, Mod. Phys. Lett. **A14** (1999) 827.
[48] D.Ashery and H.J.Lipkin, hep-ph/0002144;
D.Ashery and H.J.Lipkin, Phys. Lett. **B469** (1999) 263 [hep-ph/9908355].
[49] *originally proposed in* G.Myatt, CERN/ECFA **72-4**, Vol. II (1973) 117;
and discussed in A.Grant, Nucl. Instr. and Meth. **127** (1975) 355.
[50] S.Bentvelsen, J.Engelen, P.Kooijman, Proc. of the Workshop "Physics at HERA", edited by W.Buchmüller and G.Ingelman, DESY (1992) 23.